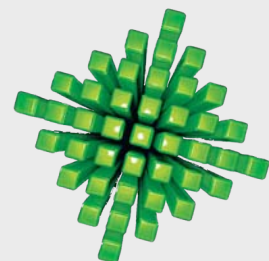


Bulk Deformation Processes

Process	General Characteristics
Forging	Production of discrete parts with a set of dies; some finishing operations usually necessary; similar parts can be made by casting and powder-metallurgy techniques; usually performed at elevated temperatures; dies and equipment costs are high; moderate to high labor costs; moderate to high operator skill.
Rolling	
Flat	Production of flat plate, sheet, and foil at high speeds, and with good surface finish, especially in cold rolling; requires very high capital investment; low to moderate labor cost.
Shape	Production of various structural shapes, such as I-beams and rails, at high speeds; includes thread and ring rolling; requires shaped rolls and expensive equipment; low to moderate labor cost; moderate operator skill.
Extrusion	Production of long lengths of solid or hollow products with constant cross-sections, usually performed at elevated temperatures; product is then cut to desired lengths; can be competitive with roll forming; cold extrusion has similarities to forging and is used to make discrete products; moderate to high die and equipment cost; low to moderate labor cost; low to moderate operator skill.
Drawing	Production of long rod, wire, and tubing, with round or various cross-sections; smaller cross-sections than extrusions; good surface finish; low to moderate die, equipment and labor costs; low to moderate operator skill.
Swaging	Radial forging of discrete or long parts with various internal and external shapes; generally carried out at room temperature; low to moderate operator skill.

TABLE 6.1 General characteristics of bulk deformation processes.



Upsetting

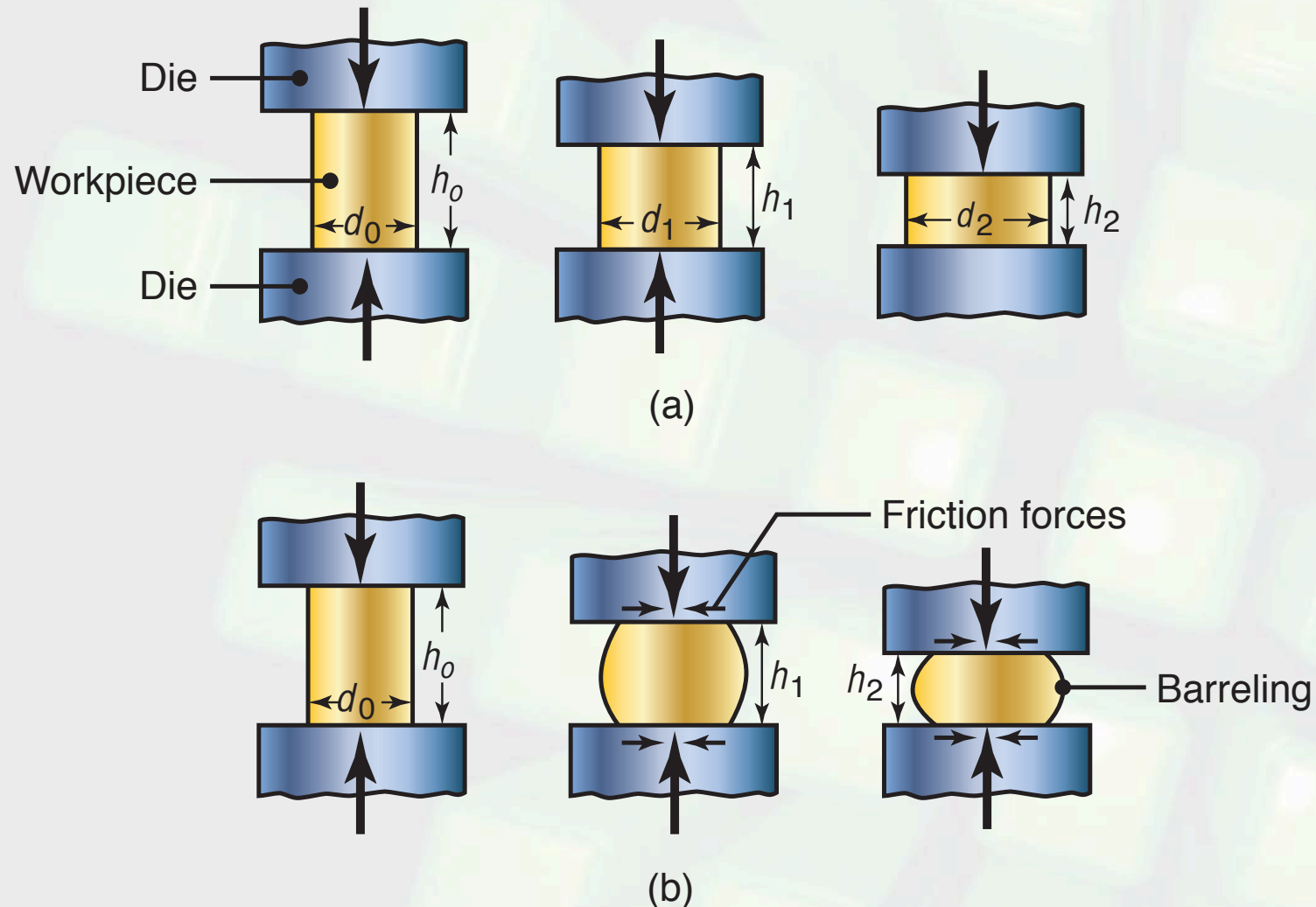
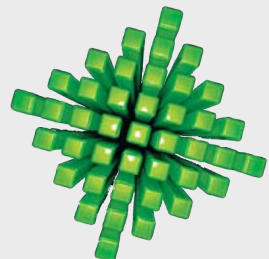


FIGURE 6.1 (a) Ideal deformation of a solid cylindrical specimen compressed between flat frictionless dies (platens), an operation known as upsetting. (b) Deformation in upsetting with friction at the die-workpiece interfaces. Note barreling of the billet caused by friction.



Grain Flow

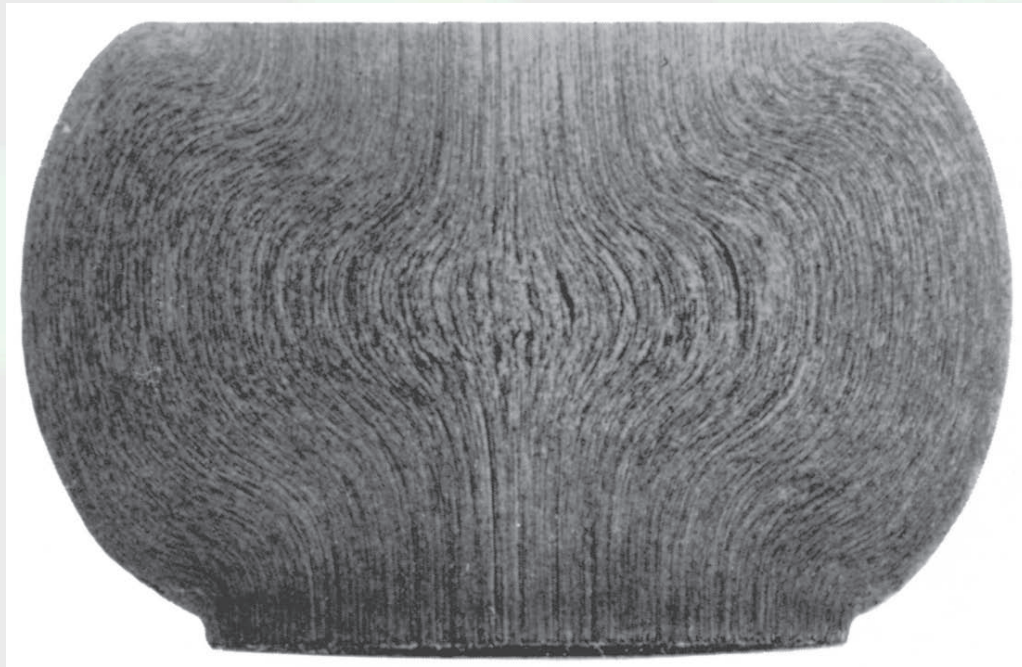


FIGURE 6.2 Grain flow lines in upsetting a solid, steel cylindrical specimen at elevated temperatures between two flat cool dies. Note the highly inhomogeneous deformation and barreling, and the difference in shape of the bottom and top sections of the specimen. The latter results from the hot specimen resting on the lower die before deformation proceeds. The lower portion of the specimen began to cool, thus exhibiting higher strength and hence deforming less than the top surface. Source: After J.A. Schey.

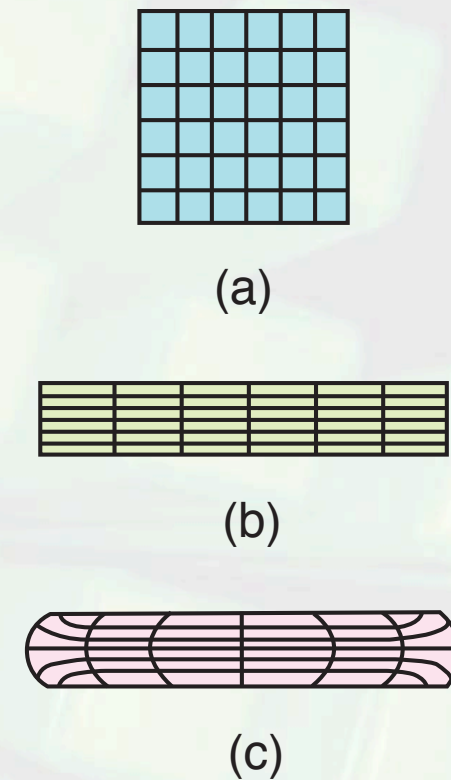
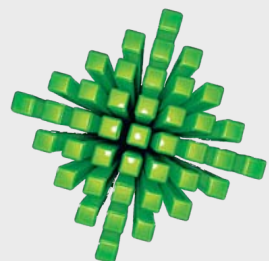


FIGURE 6.3 Schematic illustration of grid deformation in upsetting: (a) original grid pattern; (b) after deformation, without friction; (c) after deformation, with friction. Such deformation patterns can be used to calculate the strains within a deforming body.



Slab Analysis of Forging

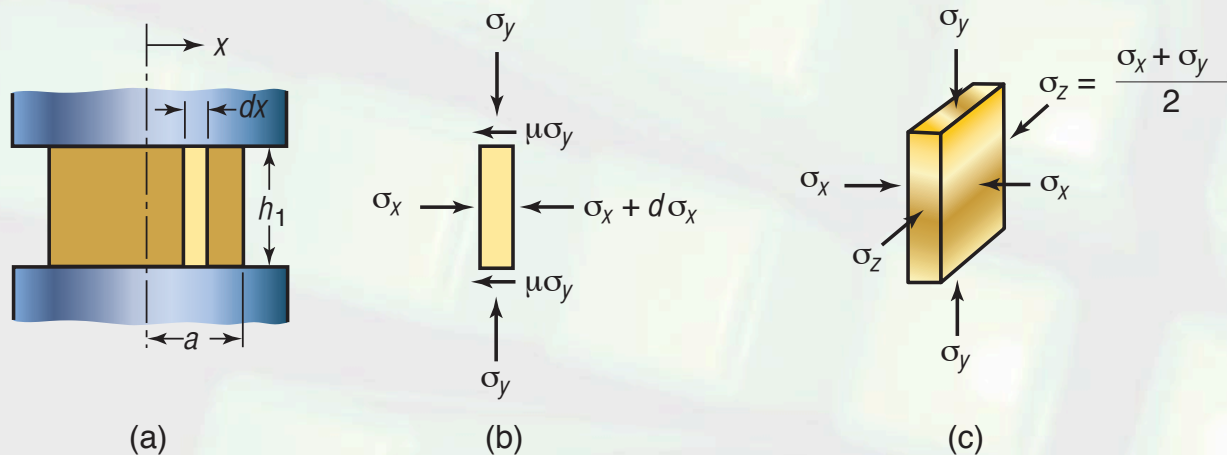


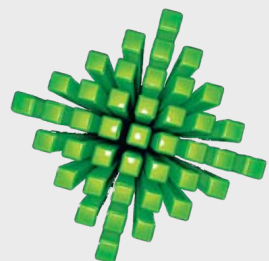
FIGURE 6.1 Stresses on an element in plane-strain compression (forging) between flat dies with friction. The horizontal stress σ_x is assumed to be uniformly distributed along the height h of the element. Identifying the stresses on an element (slab) is the first step in the slab method of analysis of metalworking processes.

From equilibrium:

$$(\sigma_x + d\sigma_x)h + 2\mu\sigma_y dx - \sigma_y h = 0$$

Resulting die pressure prediction:

$$\sigma_x = \sigma_y - Y' = Y' \left[e^{2\mu(a-x)/h} - 1 \right]$$



Die Pressure

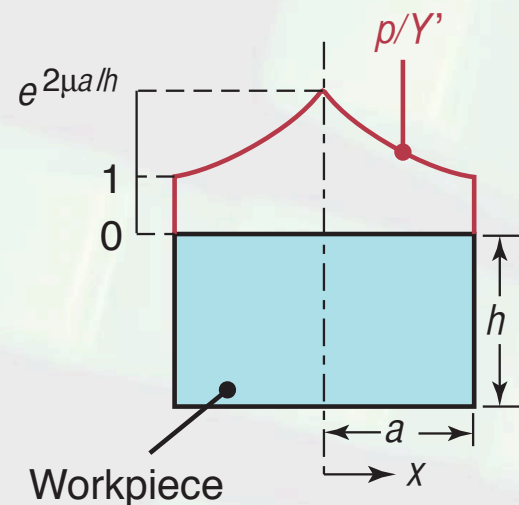


FIGURE 6.5 Distribution of die pressure, in dimensionless form of p/Y' , in plane-strain compression with sliding friction. Note that the pressure at the left and right boundaries is equal to the yield stress of the material in plane strain, Y' . Sliding friction means that the frictional stress is directly proportional to the normal stress.

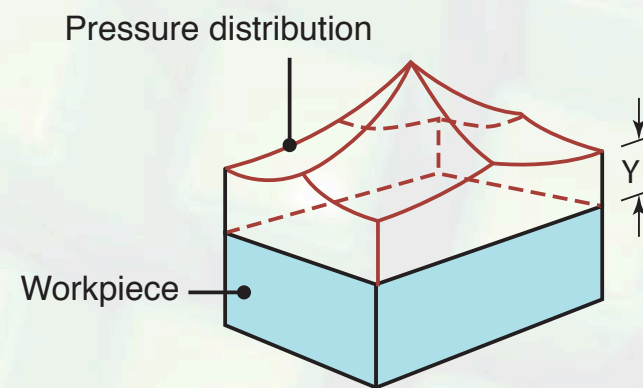


FIGURE 6.6 Die pressure distribution in compressing a rectangular workpiece with sliding friction and under conditions of plane stress, using the *distortion-energy criterion*. Note that the stress at the corners is equal to the uniaxial yield stress, Y , of the material.

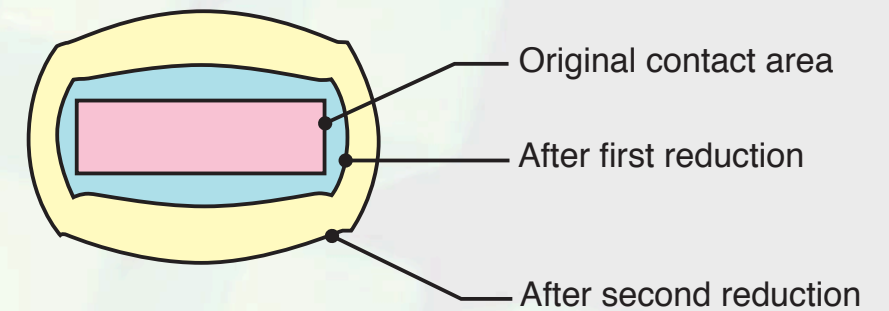
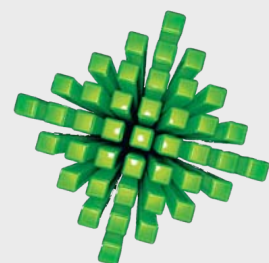
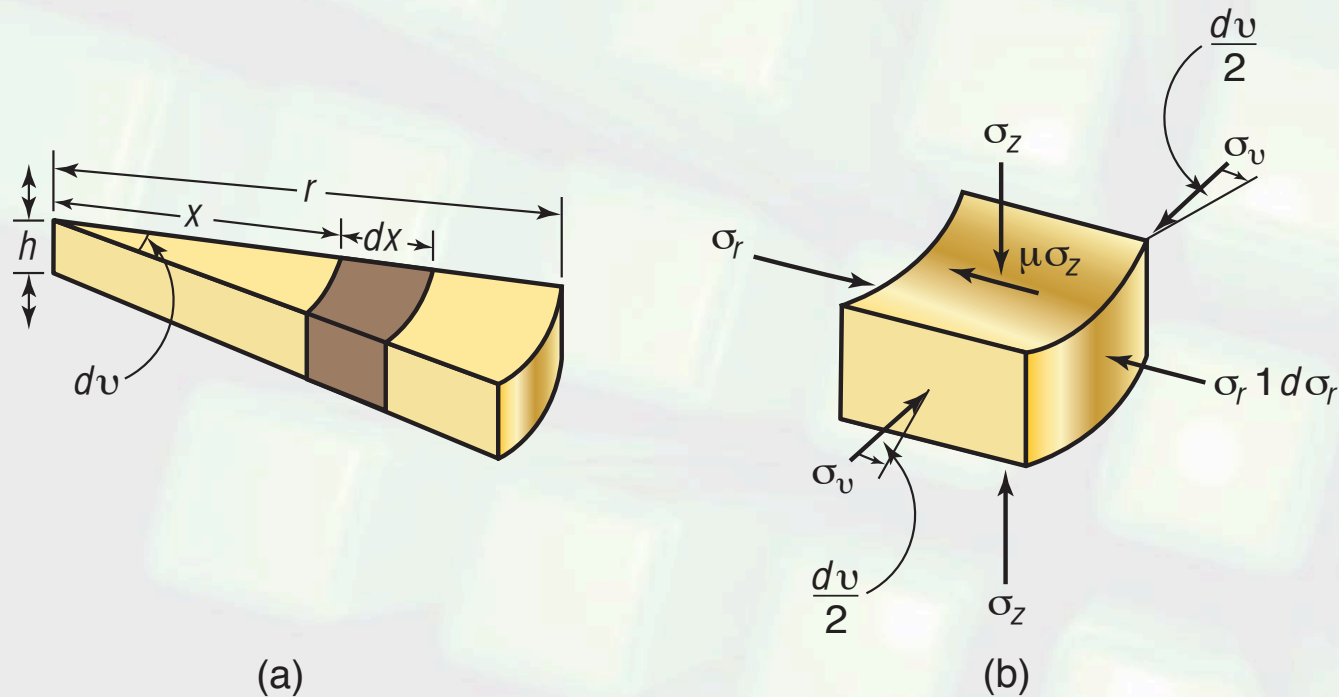


FIGURE 6.7 Increase in die-workpiece contact area of an originally rectangular specimen (viewed from the top) compressed between flat dies and with friction. Note that the length of the specimen (horizontal dimension) has increased proportionately less than its width (vertical dimension). Likewise, a specimen originally in the shape of a cube acquires the shape of a pancake after deformation with friction.



Slab Method for Cylindrical Workpiece



Results:

$$p = Y e^{2\mu(r-x)/h}.$$

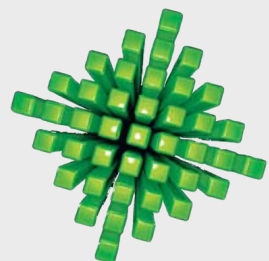
Average pressure:

$$p_{av} \simeq Y \left(1 + \frac{2\mu r}{3h} \right).$$

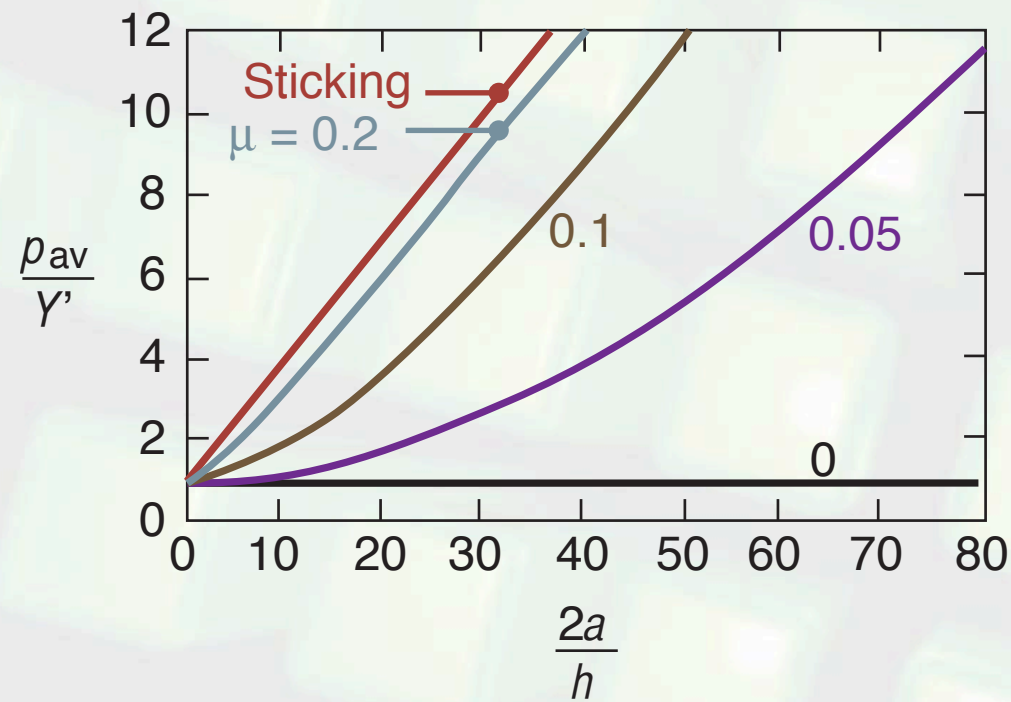
Forging force:

$$F = (p_{av}) (\pi r^2)$$

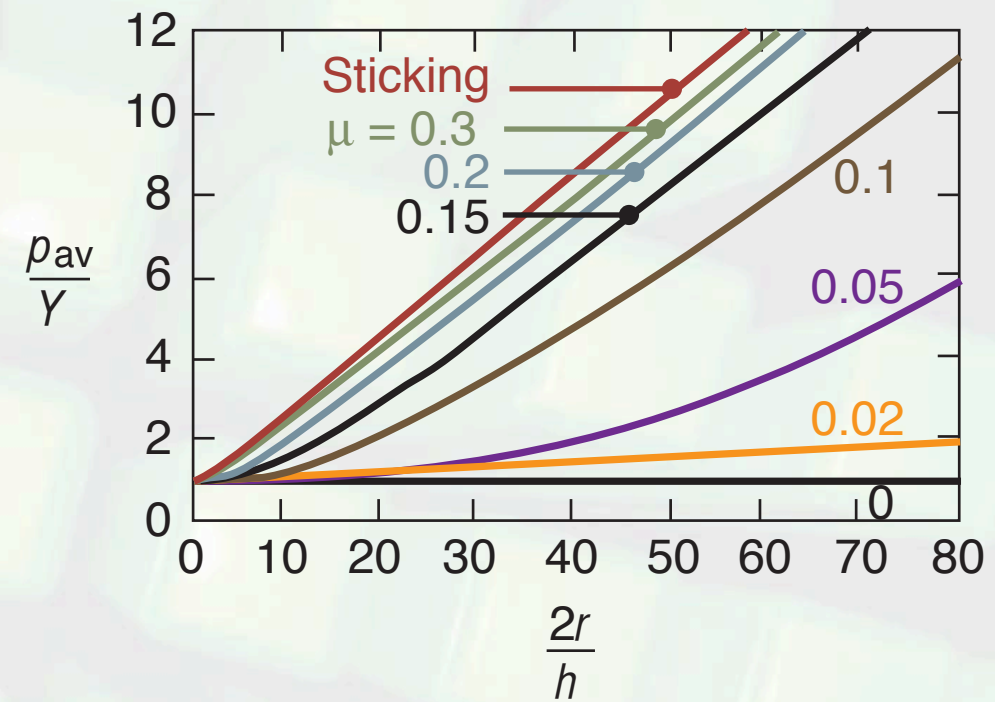
FIGURE 6.8 Stresses on an element in forging of a solid cylindrical workpiece between flat dies and with friction. Compare this figure and the stresses involved with Fig. 6.4.



Die Pressure

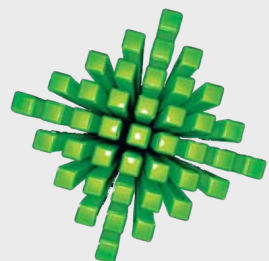


(a)

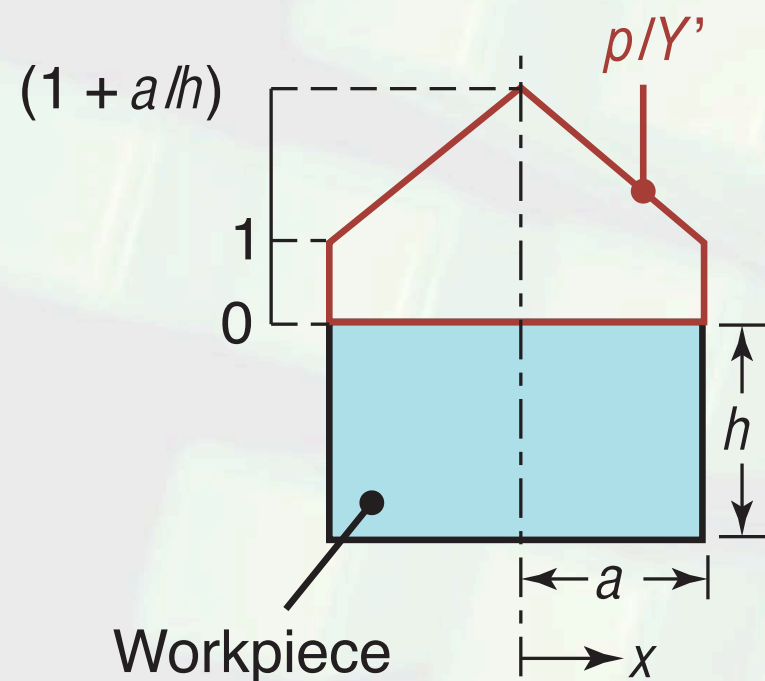


(b)

FIGURE 6.9 Ratio of average die pressure to yield stress as a function of friction and aspect ratio of the specimen: (a) plane-strain compression; and (b) compression of a solid cylindrical specimen. Note that the yield stress in (b) is Y , and not Y' as it is in the plane-strain compression shown in (a). Source: After J.F.W. Bishop.



Pressure with Sticking Condition



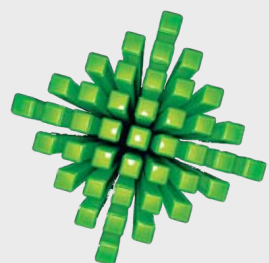
Results for sticking friction in plane strain:

$$p = Y' \left(1 + \frac{a - x}{h} \right)$$

Results for sticking friction with cylinder:

$$p = Y \left(1 + \frac{r - x}{h} \right)$$

FIGURE 6.10 Distribution of dimensionless die pressure, p/Y' , in compressing a rectangular specimen in plane strain and under sticking conditions. Sticking means that the frictional (shear) stress at the interface has reached the shear yield stress of the material. Note that the pressure at the edges is the uniaxial yield stress of the material in plane strain, Y' .



Finite Element Analysis

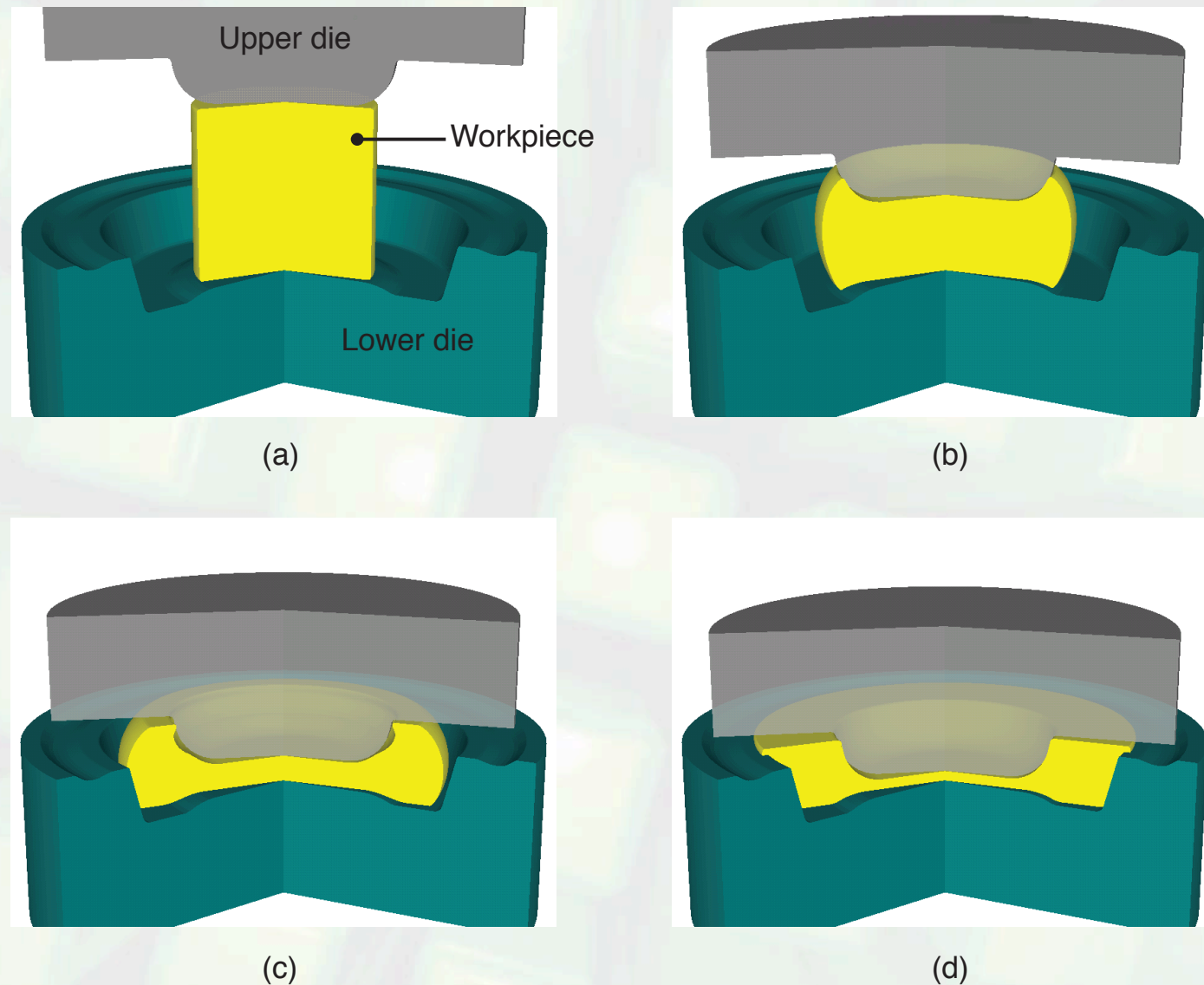
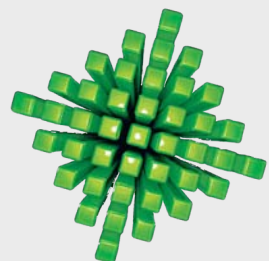


FIGURE 6.11 Deformation of a blank during forging as predicted by the software program DEFORM based on the finite-element method of analysis. *Source:* Courtesy Scientific Forming Technologies Corporation.



Die Pressure and Aspect Ratio

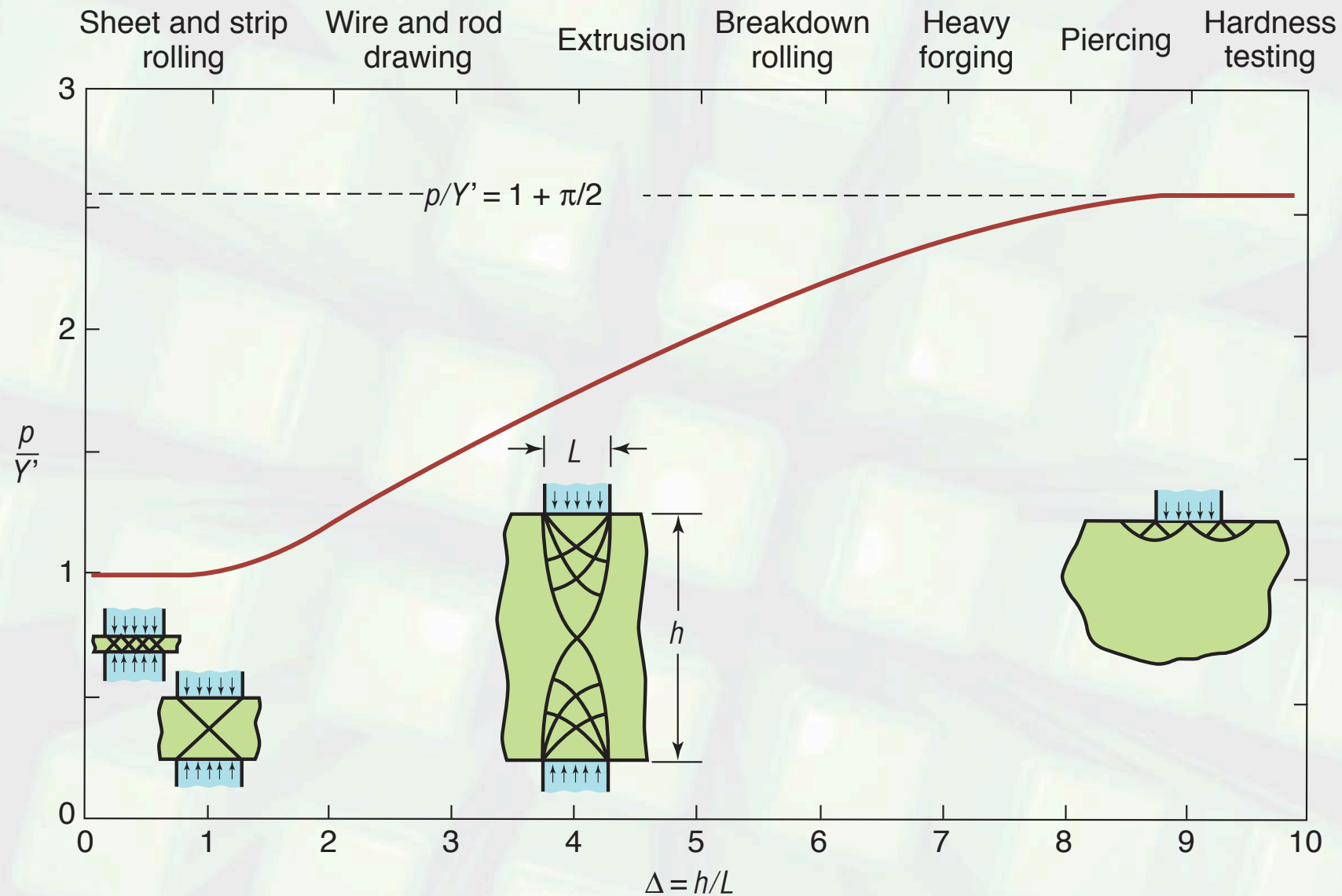
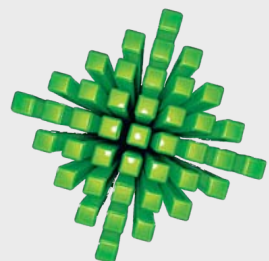


FIGURE 6.12 Die pressure required in various metalworking operations and under *frictionless* plane-strain conditions, as obtained by the slip-line analysis. Note that the magnitude of the die-workpiece contact area is an important factor in determining pressures. Source: After W.A. Backofen.



Plane Strain Examples

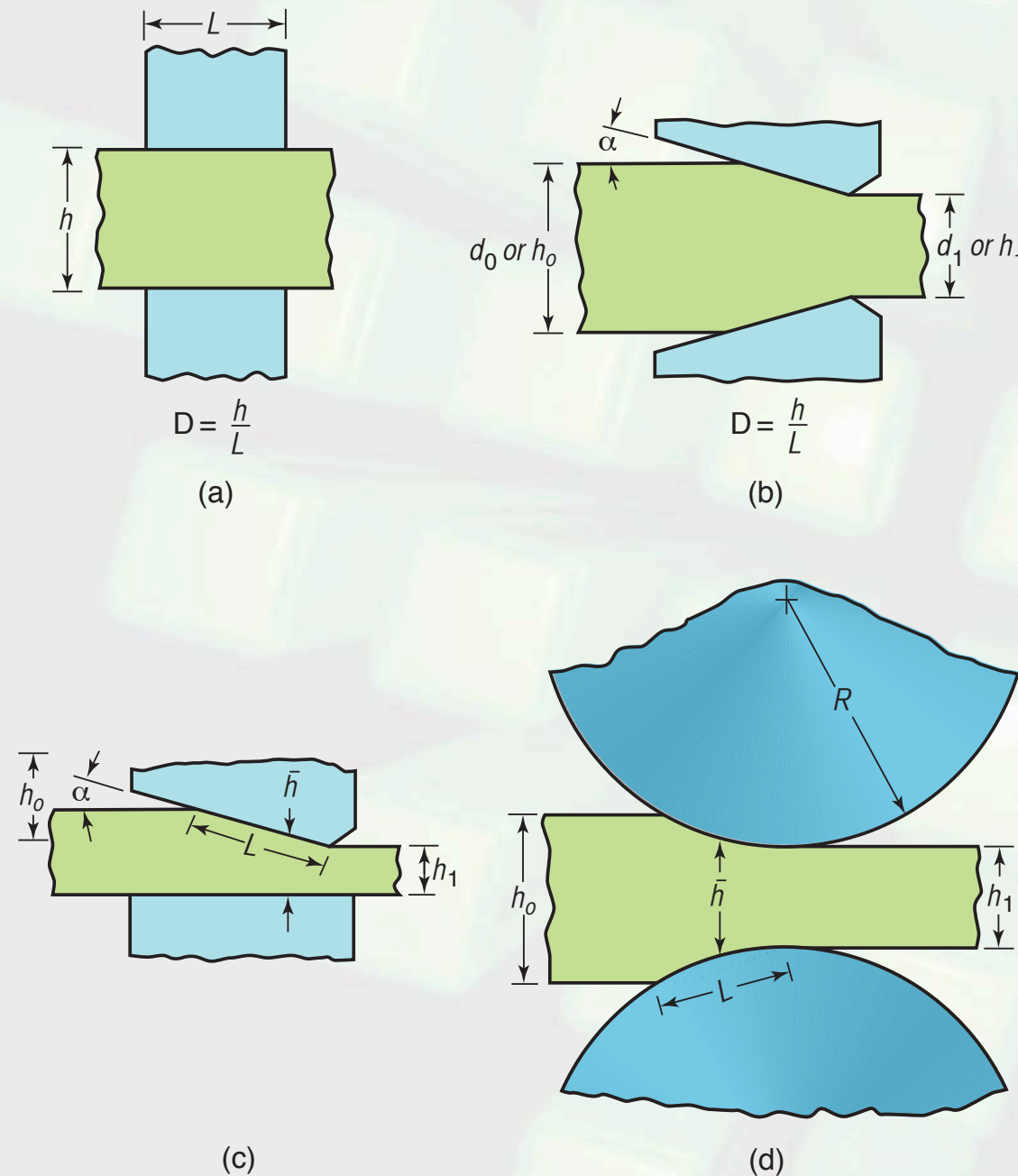
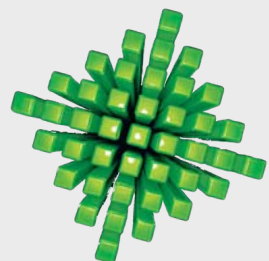


FIGURE 6.13 Examples of plastic deformation processes in plane strain, showing the h/L ratio. (a) Indenting with flat dies, an operation similar to the cogging process, as shown in Fig. 6.19. (b) Drawing or extrusion of a strip with a wedge-shaped die, as described in Sections 6.4 and 6.5. (c) Ironing; see also 7.53. (d) Rolling, described in Section 6.3.



Impression Die Forging

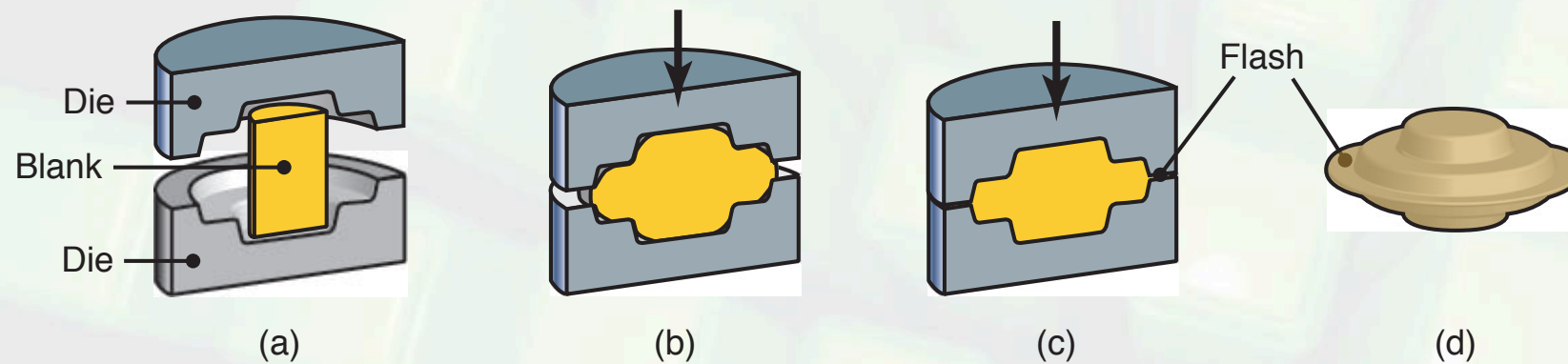


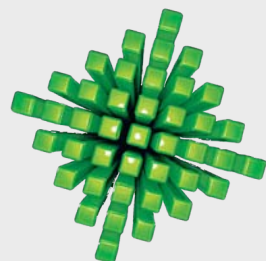
FIGURE 6.14 Schematic illustrations of stages in impression-die forging. Note the formation of a flash, or excess material that subsequently has to be trimmed off.

TABLE 6.2 Range of K_p values in Eq. (6.22) for impression-die forging.

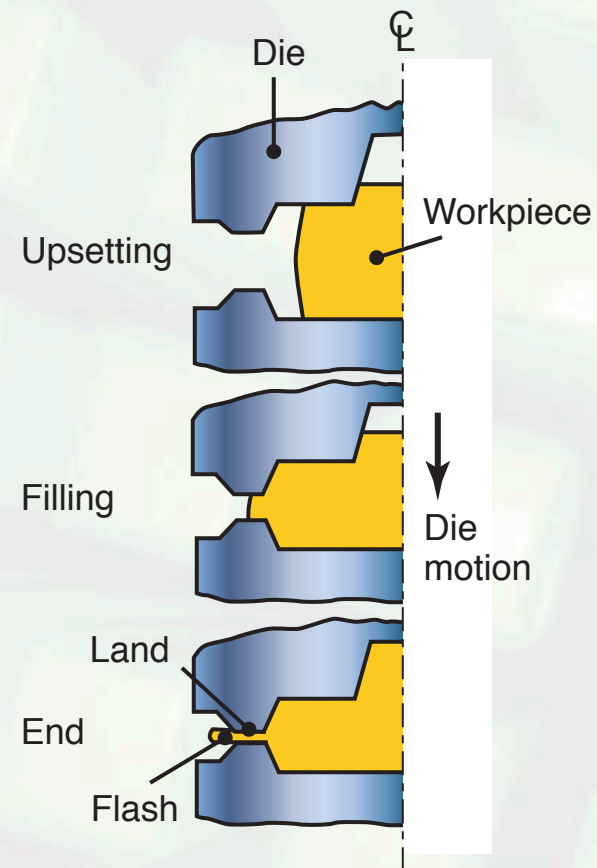
Simple shapes, without flash	3-5
Simple shapes, with flash	5-8
Complex shapes, with flash	8-12

Forging force:

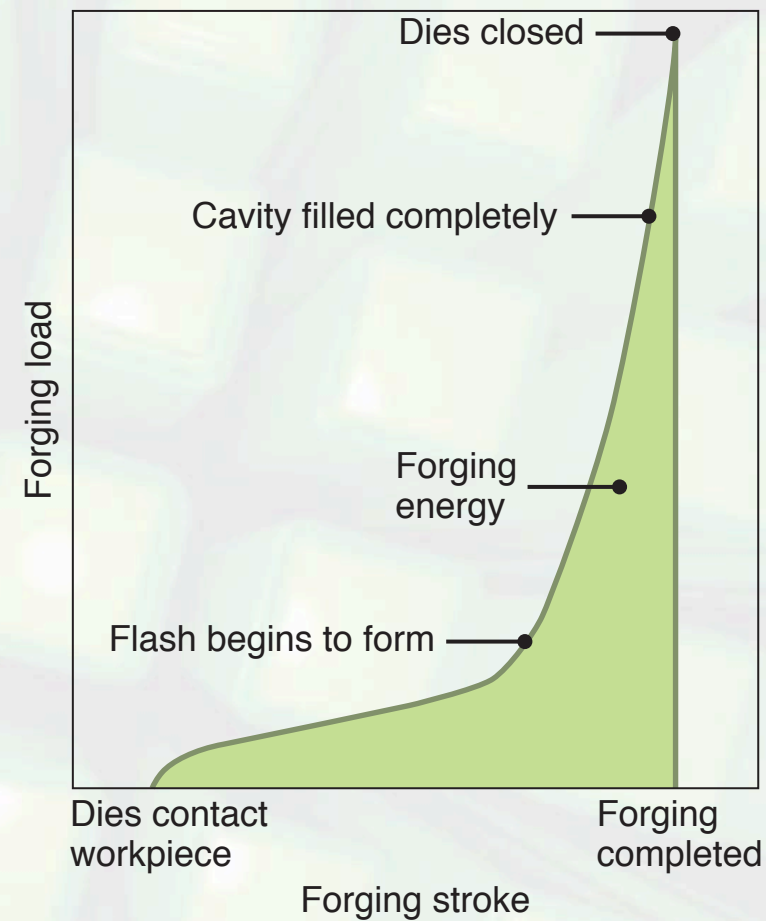
$$F = K_p Y_f A$$



Load-Stroke Curve

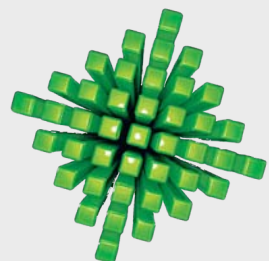


(a)



(b)

FIGURE 6.15 Typical load-stroke curve for impression-die forging. Note the sharp increase in load when the flash begins to form. Source: After T.Altan.



Orbital-Forging

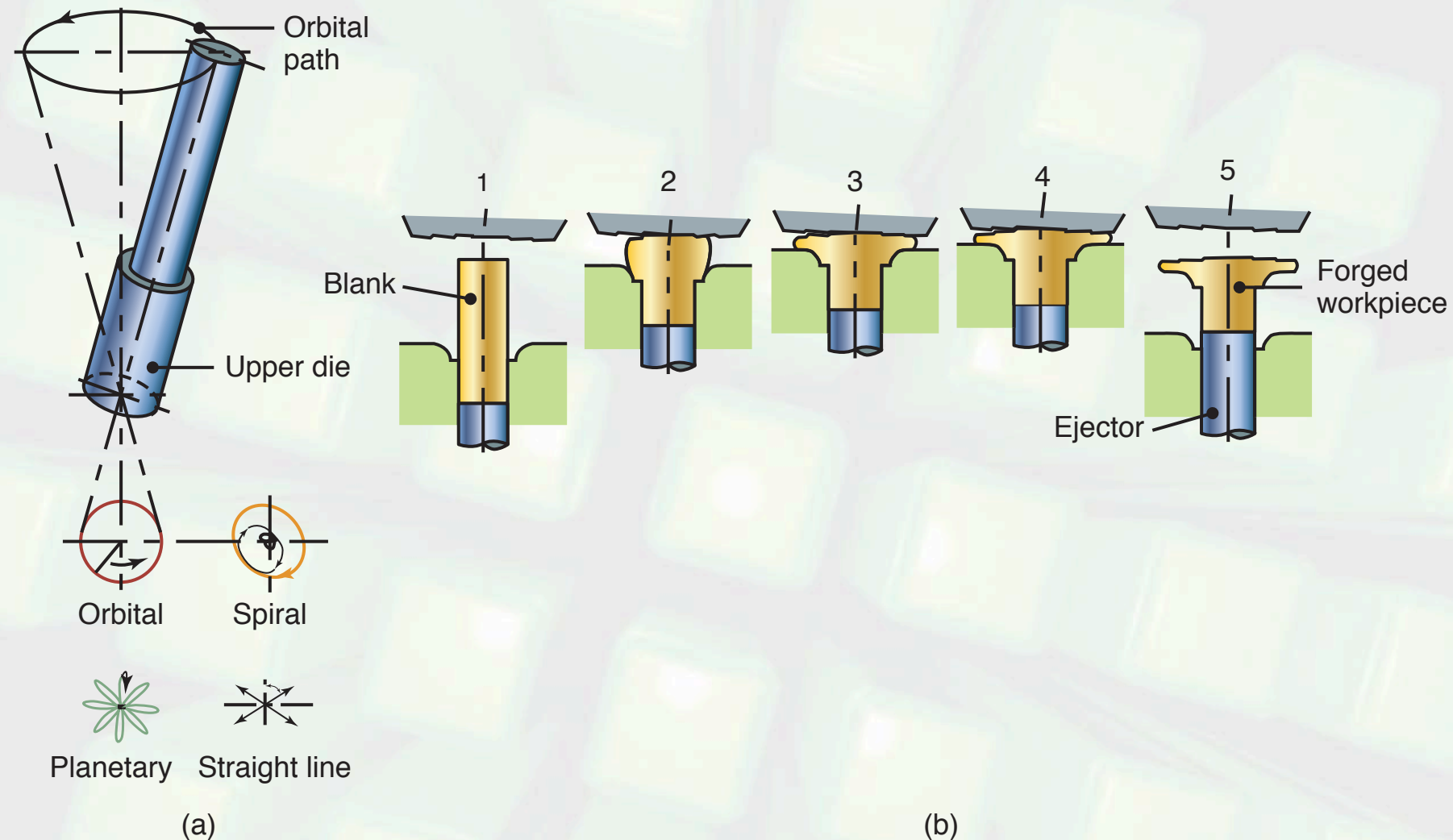
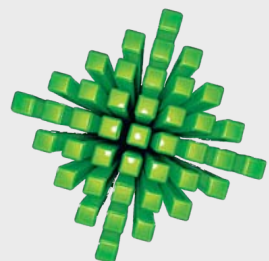


FIGURE 6.16 Schematic illustration of the orbital-forging process. Note that the die is in contact with only a portion of the workpiece surface at a time. Also called *rotary forging*, *swing forging*, and *rocking-die forging*, this process can be used for forming individual parts such as bevel gears, wheels, and bearing rings.



Heading & Piercing

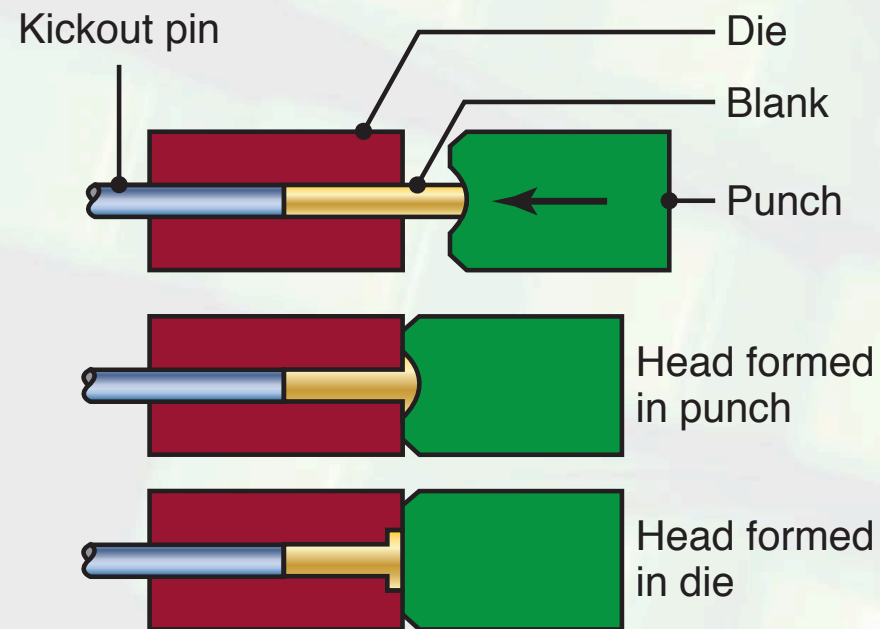


FIGURE 6.17 Forming the heads of fasteners, such as bolts and rivets, by the *heading* process.

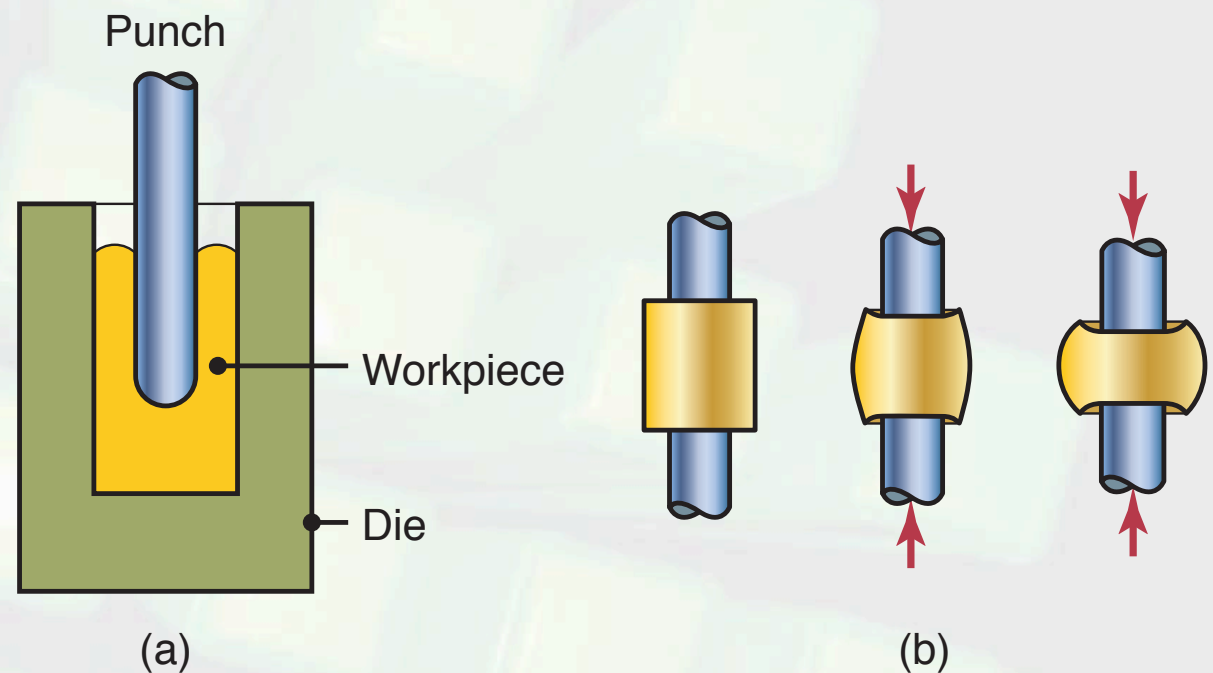
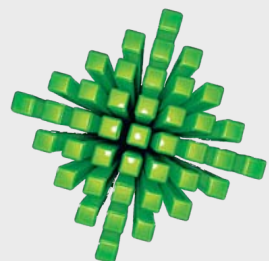


FIGURE 6.18 Examples of piercing operations.



Open-Die Forging

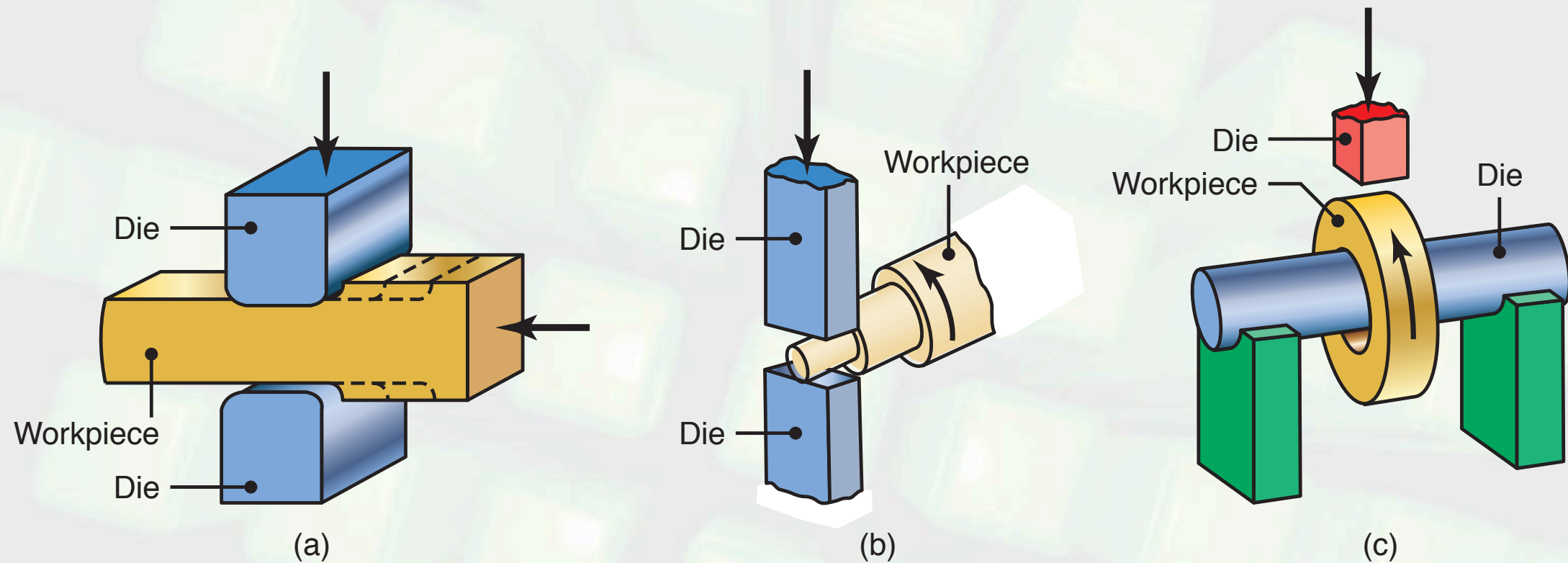
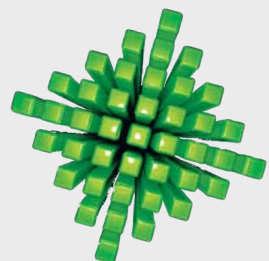


FIGURE 6.19 (a) Schematic illustration of a cogging operation on a rectangular bar. Blacksmiths use a similar procedure to reduce the thickness of parts in small increments by heating the workpiece and hammering it numerous times along the length of the part. (b) Reducing the diameter of a bar by open-die forging; note the movements of the die and the workpiece. (c) The thickness of a ring being reduced by open-die forging.



Roll Forging

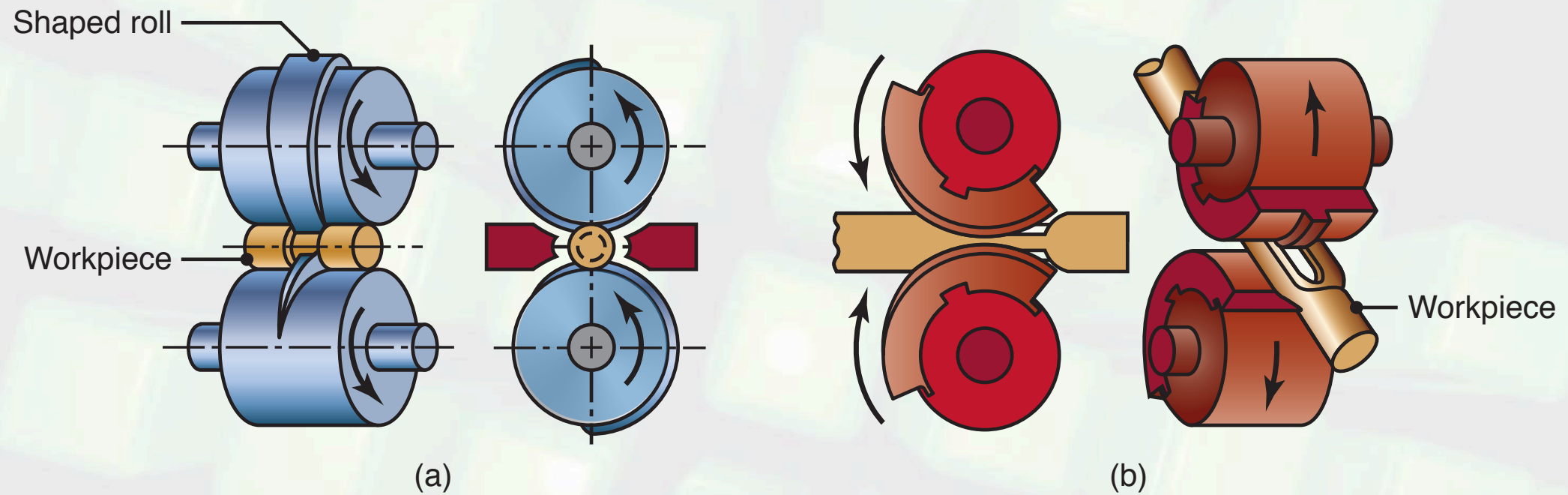
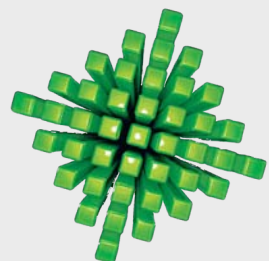


FIGURE 6.21 Two illustrations of roll forging (*cross-rolling*) operations. Tapered leaf springs and knives can be made by this process using specially designed rolls. Source: After J. Holub.



Production of Ball Bearings

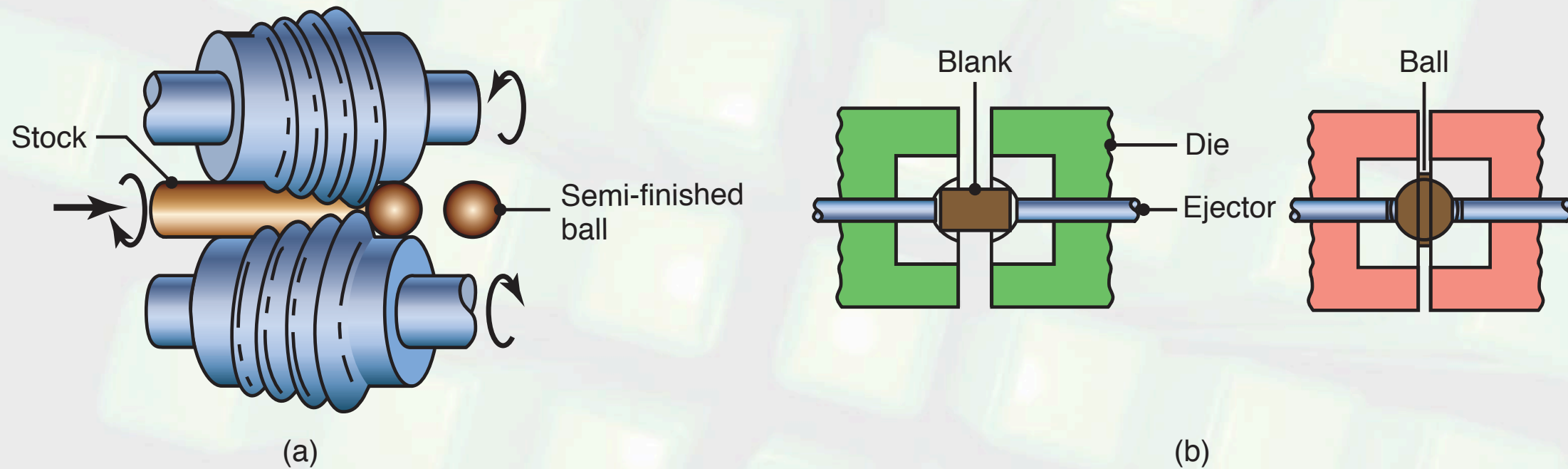
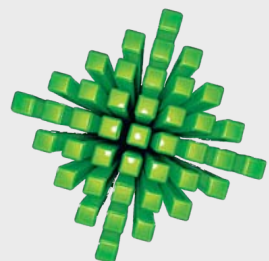


FIGURE 6.21 (a) Production of steel balls for bearings by skew rolling. (b) Production of steel balls by upsetting of a short cylindrical blank; note the formation of flash. The balls are subsequently ground and polished to be used as ball bearings and similar components.



Forging Defects

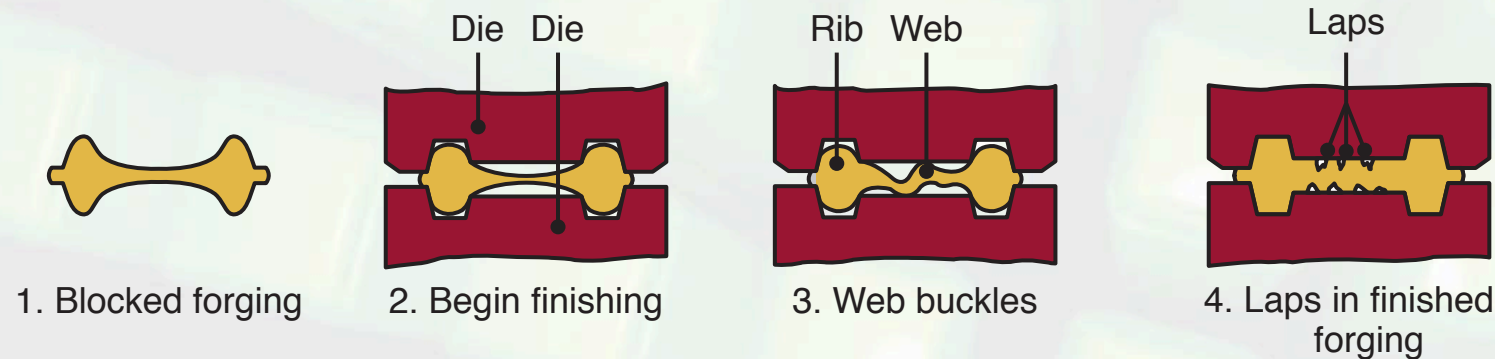
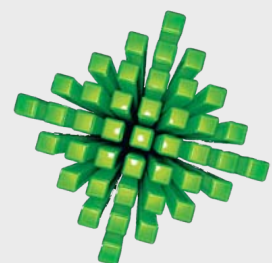
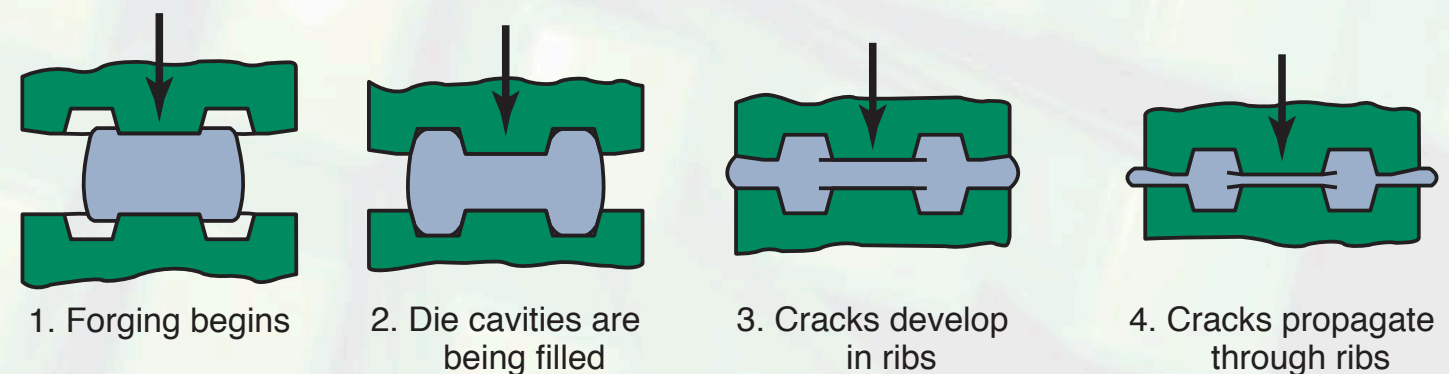


FIGURE 6.22 Stages in lap formation in a part during forging, due to buckling of the web. Web thickness should be increased to avoid this problem.

FIGURE 6.23 Stages in internal defect formation in a forging because of an oversized billet. The die cavities are filled prematurely, and the material at the center of the part flows radially outward and past the filled regions as deformation continues.



Effect of Radius

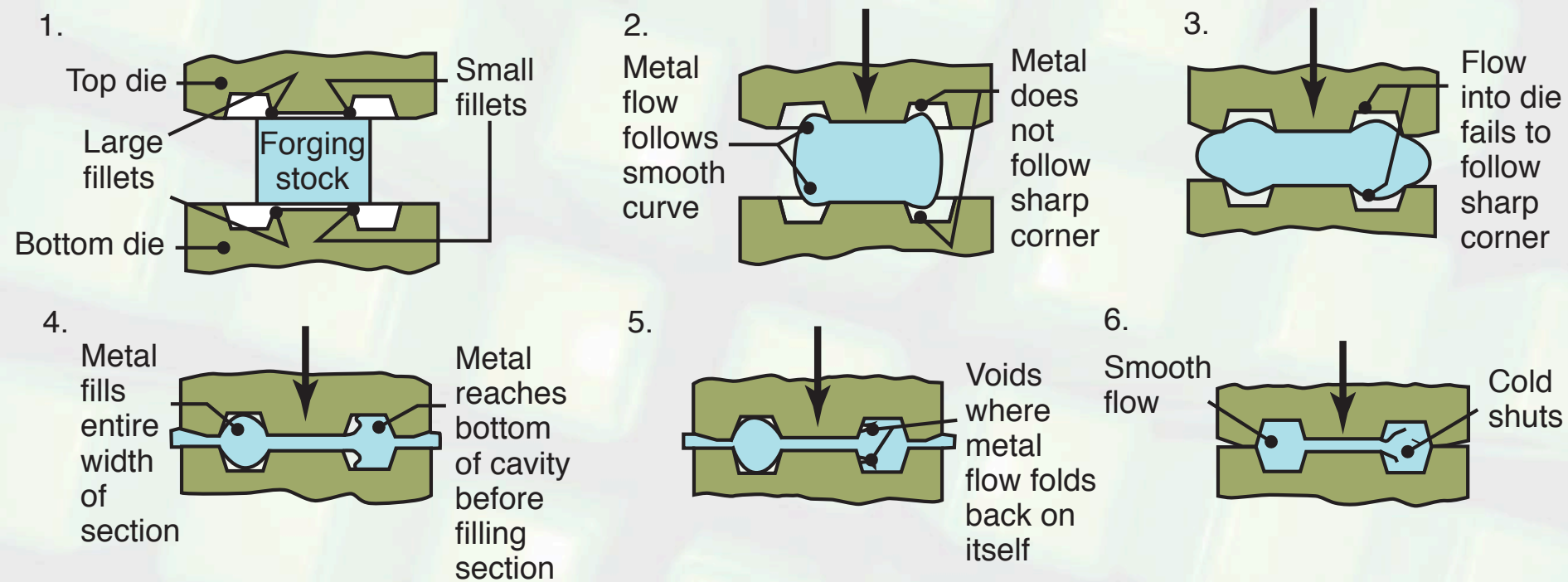
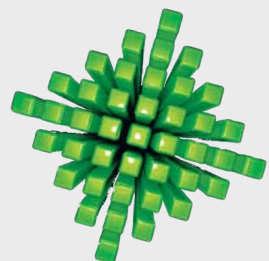


FIGURE 6.24 Effect of fillet radius on defect formation in forging. Note that small fillets (right side of the drawings) lead to defects. Source: Aluminum Company of America.



Forging Dies

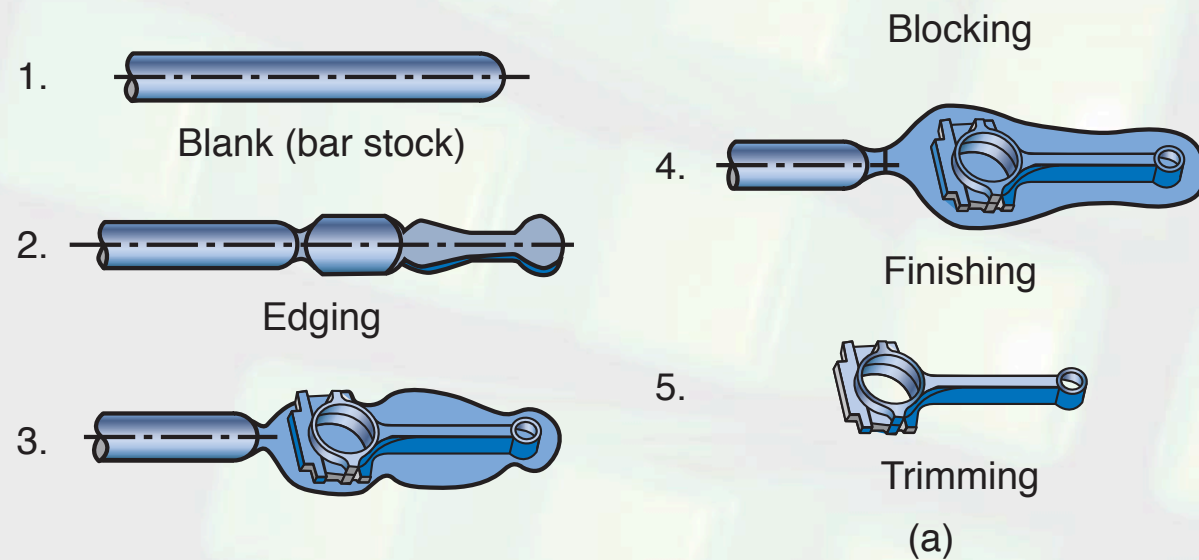


FIGURE 6.25 Stages in forging a connecting rod for an internal combustion engine. Note the amount of flash developed, which is important in properly filling die cavities.

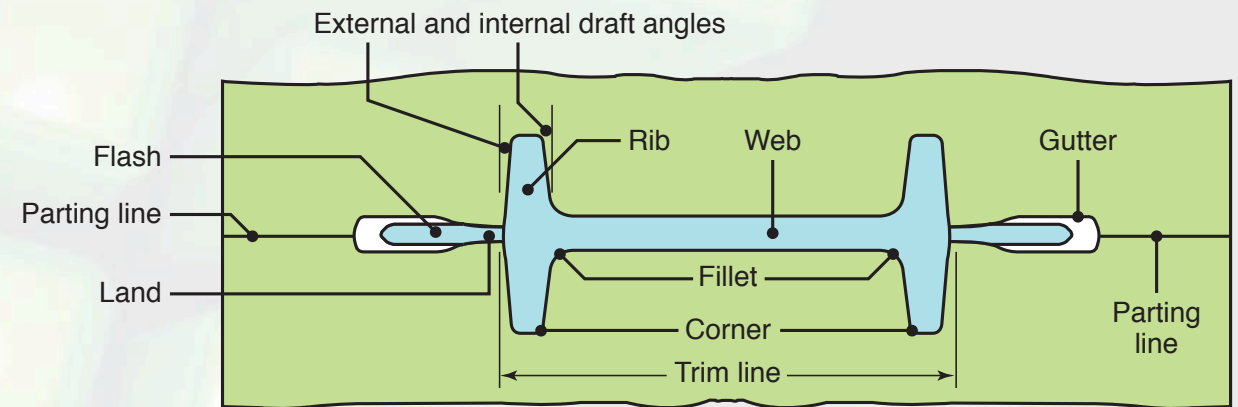
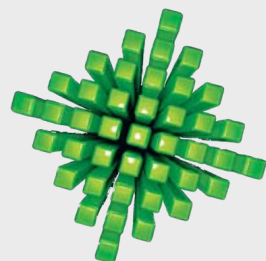


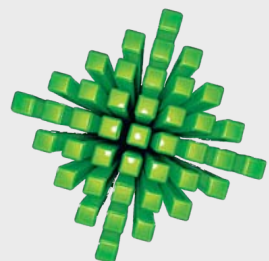
FIGURE 6.26 Standard terminology for various features of a typical forging die.



Forging Temperatures

Metal	°C	°F
Aluminum alloys	400-450	750-850
Copper alloys	625-950	1150-1750
Nickel alloys	870-1230	1600-2250
Alloy steels	925-1260	1700-2300
Titanium alloys	750-795	1400-1800
Refractory alloys	975-1650	1800-3000

TABLE 6.3 Forging temperature ranges for various metals.



Metalworking Equipment

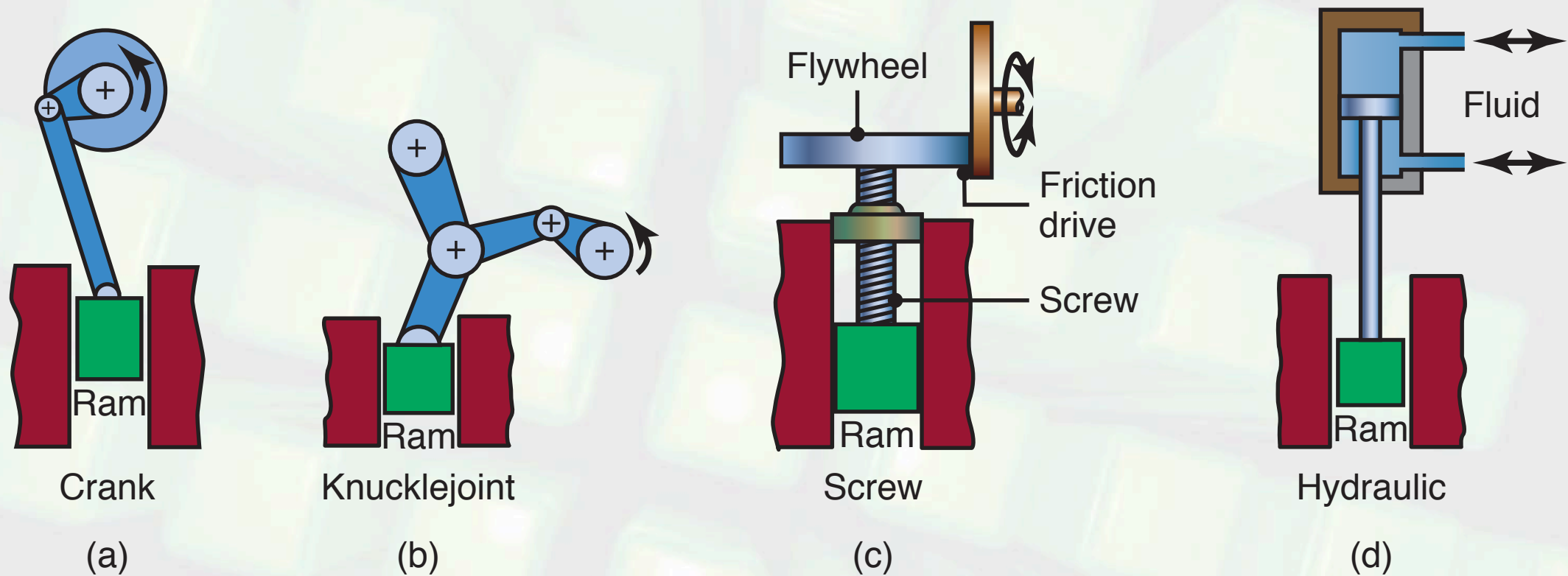
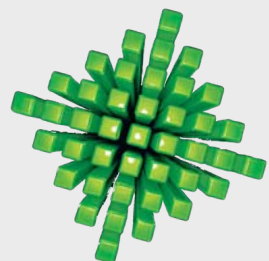


FIGURE 6.27 Schematic illustration of various types of presses used in metalworking. The choice of a press is an important consideration in the overall operation and productivity.



Rolling Operations

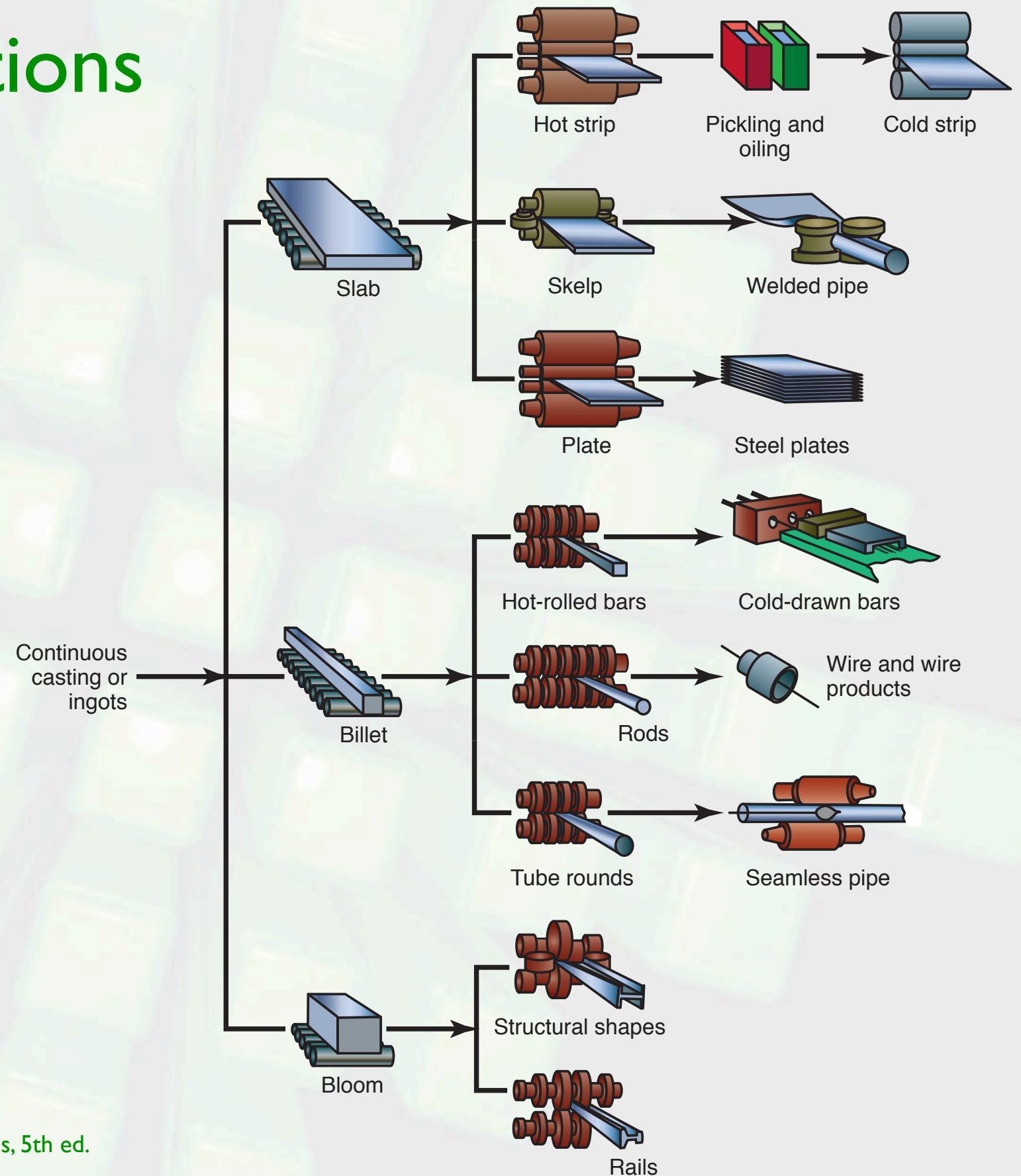
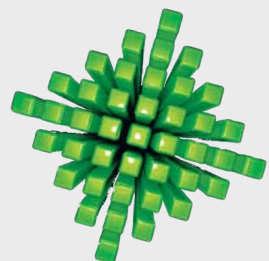


FIGURE 6.28 Schematic outline of various flat-rolling and shape-rolling operations.
Source: American Iron and Steel Institute.



Grain Structure in Hot Rolling

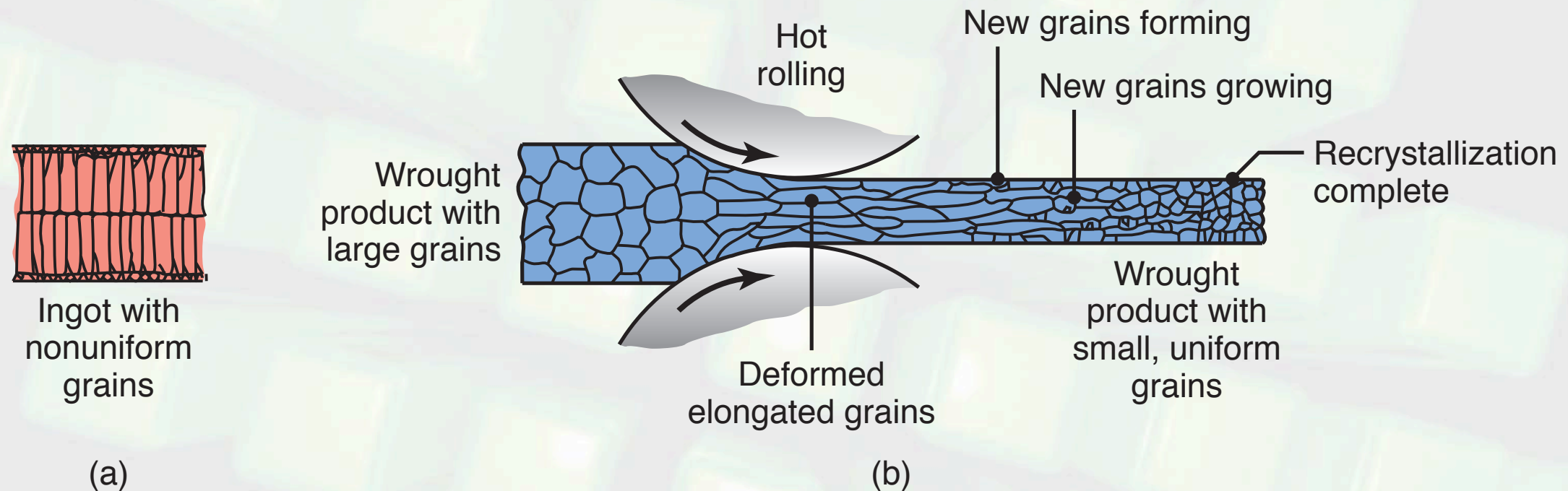
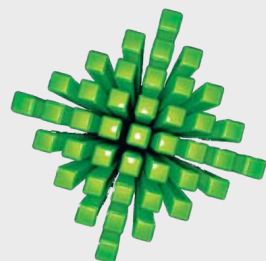


FIGURE 6.29 Changes in the grain structure of metals during hot rolling. This is an effective method to reduce grain size and refine the microstructure in metals, resulting in improved strength and good ductility. In this process cast structures of ingots or continuous castings are converted to a wrought structure.



Mechanics of Rolling

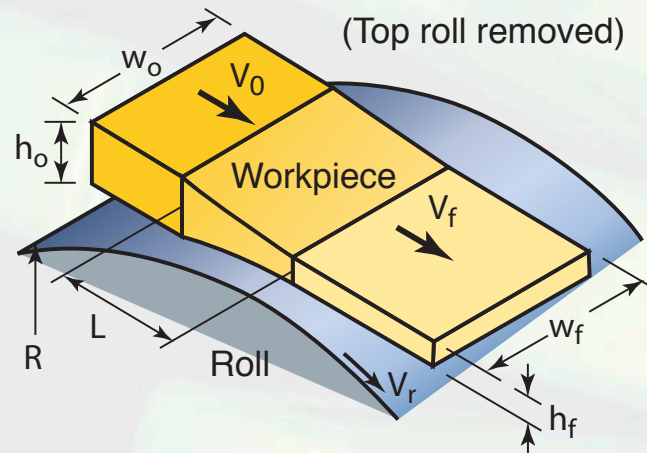


FIGURE 6.30 Schematic illustration of the flat-rolling process. (Note that the top roll has been removed for clarity.)

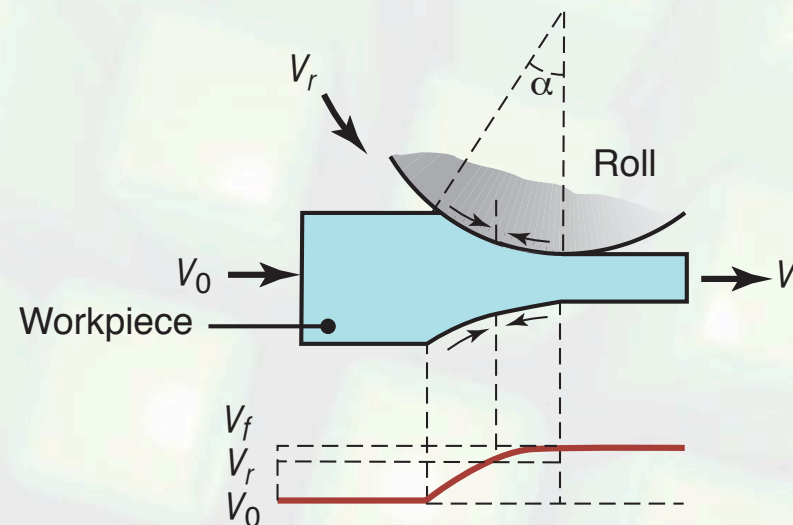
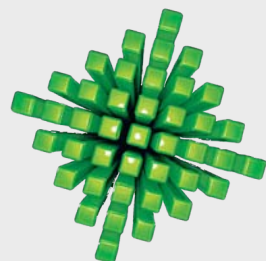


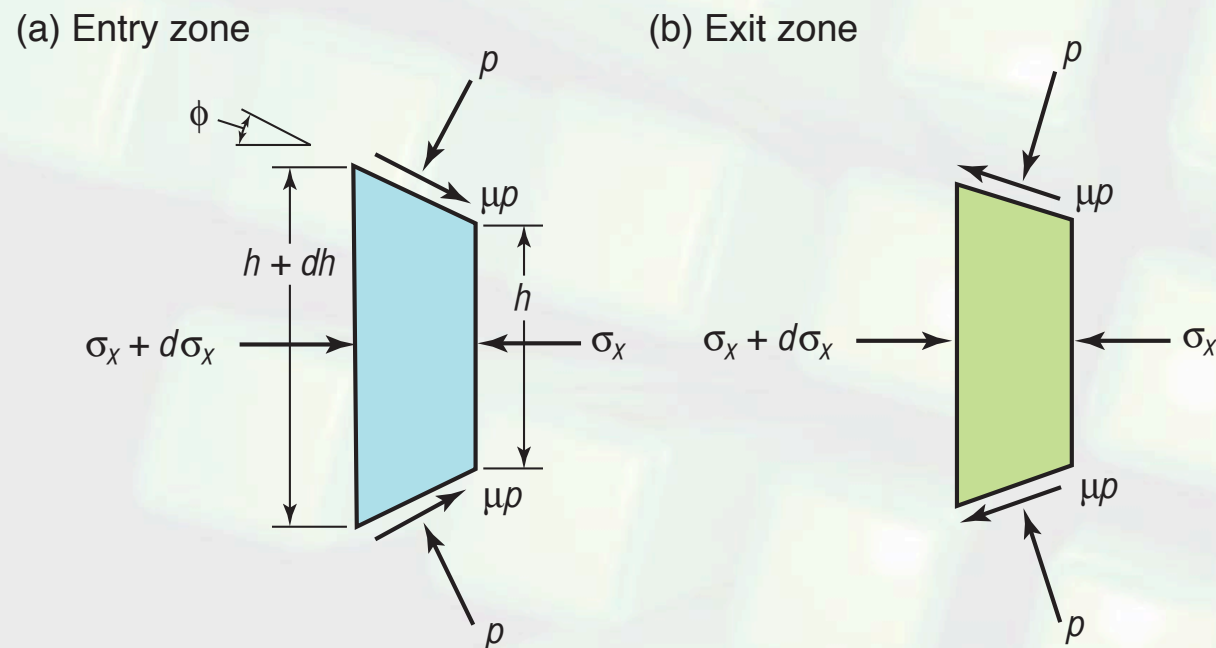
FIGURE 6.31 Relative velocity distribution between roll and strip surfaces. The arrows represent the frictional forces acting along the strip-roll interfaces. Note the difference in their direction in the left and right regions.

Forward slip:

$$\text{Forward slip} = \frac{V_f - V_r}{V_r}$$



Slab Method for Rolling



Entry zone pressure:

$$p = Y'_f \frac{h}{h_0} e^{\mu(H_0 - H)}$$

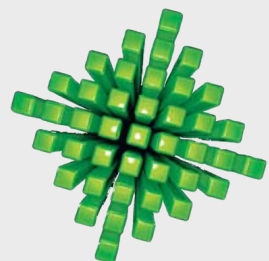
Exit zone pressure:

$$p = Y'_f \frac{h}{h_f} e^{\mu H}$$

where

$$H = 2 \sqrt{\frac{R}{h_f}} \tan^{-1} \left(\sqrt{\frac{R}{h_f}} \phi \right)$$

FIGURE 6.32 Stresses acting on an element in rolling: (a) entry zone and (b) exit zone.



Pressure Distribution in Rolling

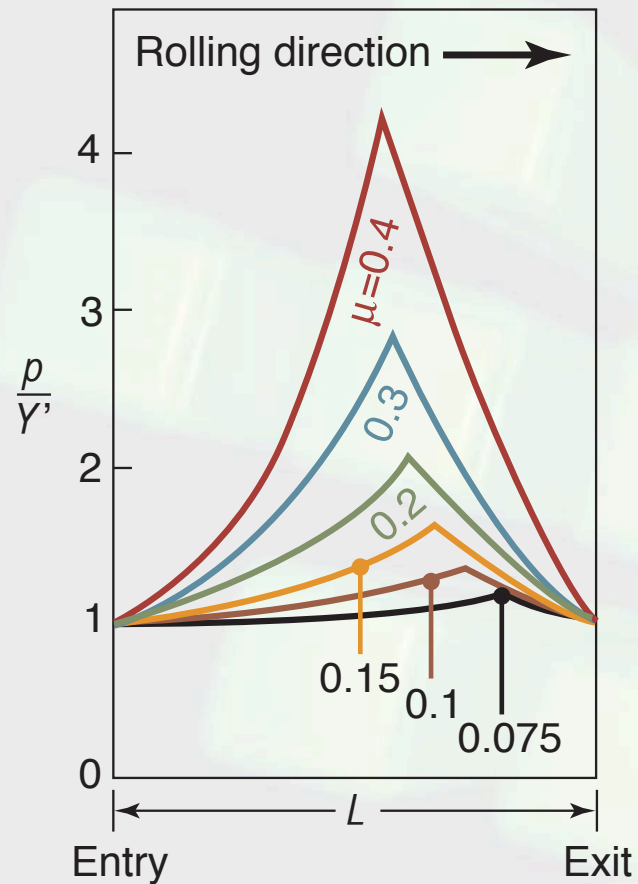


FIGURE 6.33 Pressure distribution in the roll gap as a function of the coefficient of friction. Note that as friction increases, the neutral point shifts toward the entry. Without friction, the rolls will slip, and the neutral point shifts completely to the exit. (See also Table 4.1.)

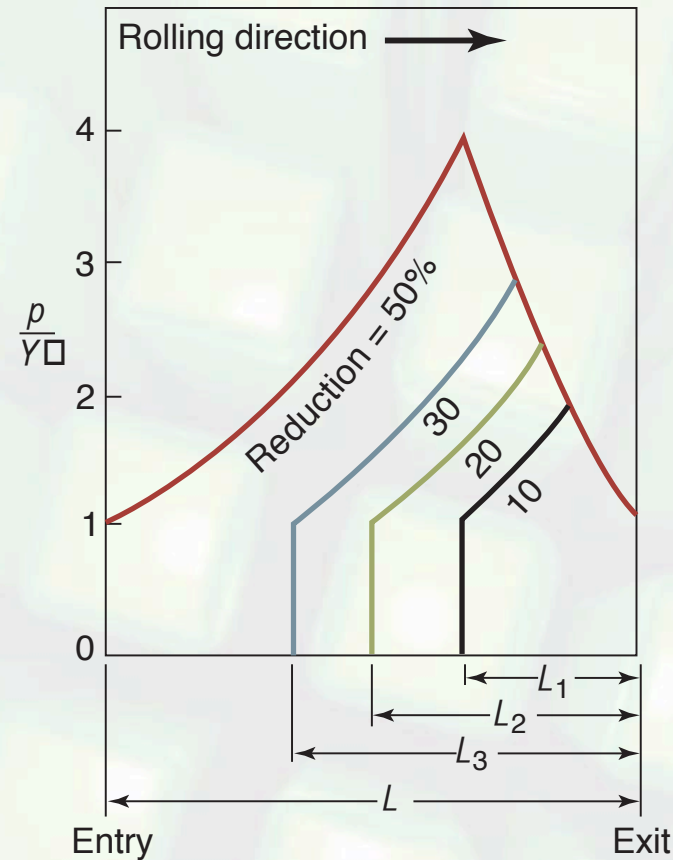


FIGURE 6.34 Pressure distribution in the roll gap as a function of reduction in thickness. Note the increase in the area under the curves with increasing reduction, thus increasing the roll force.

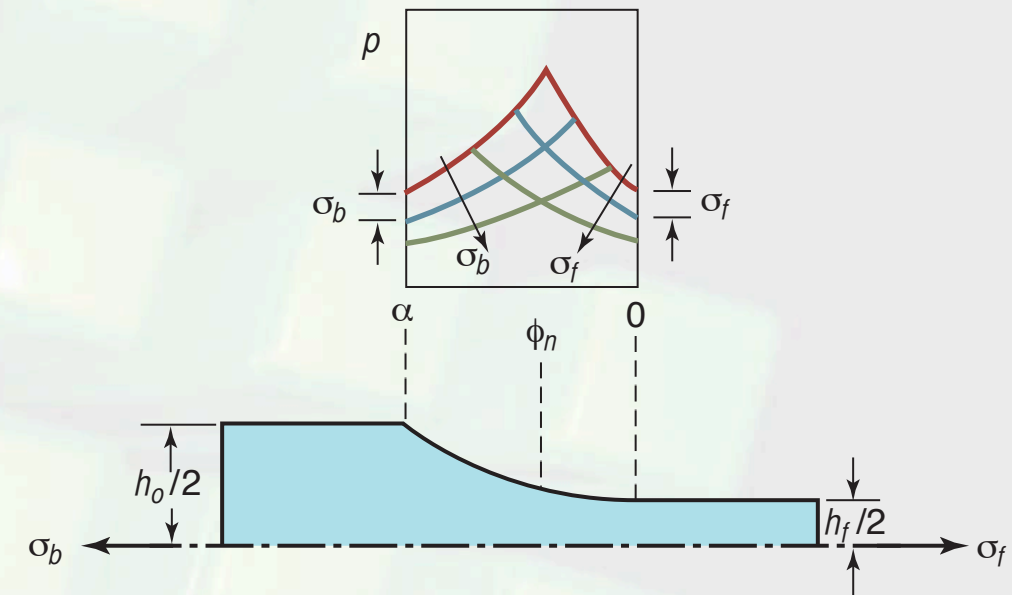
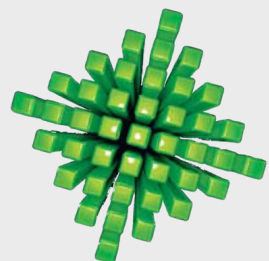


FIGURE 6.35 Pressure distribution as a function of front and back tension in rolling. Note the shifting of the neutral point and the reduction in the area under the curves (hence reduction in the roll force) as tensions increase.



Roll Bending & Slab Spread

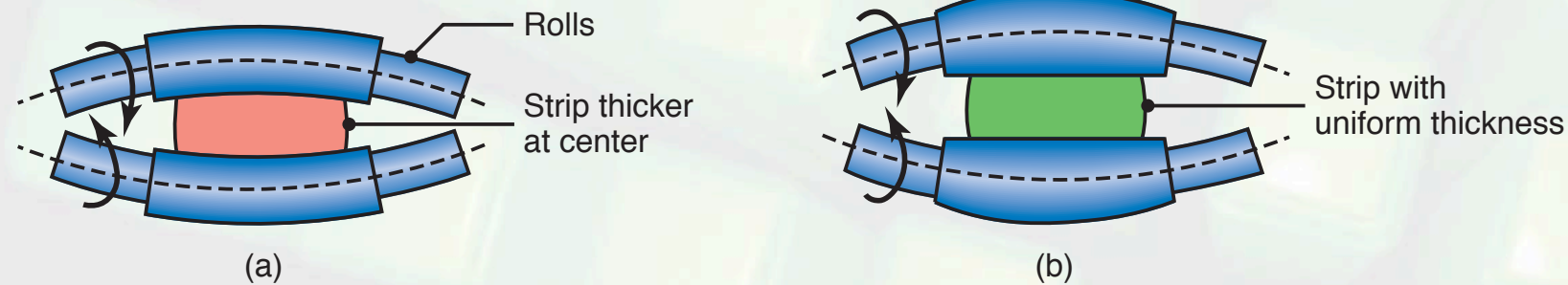


FIGURE 6.36 (a) Bending of straight cylindrical rolls (exaggerated) because of the roll force. (b) Bending of rolls, ground with camber, that produce a sheet of uniform thickness during rolling.

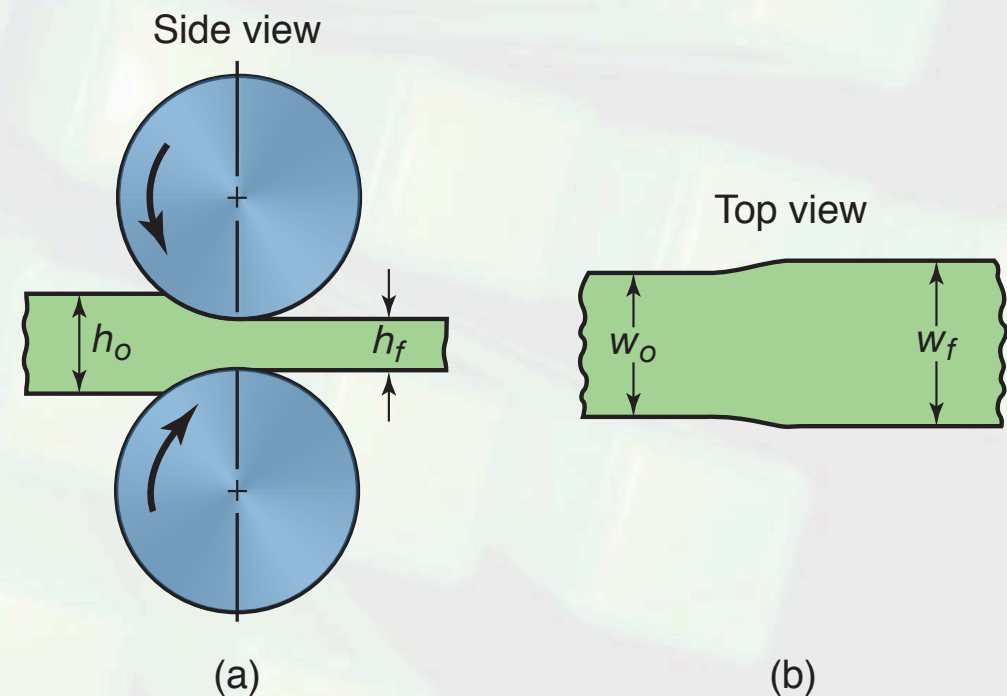
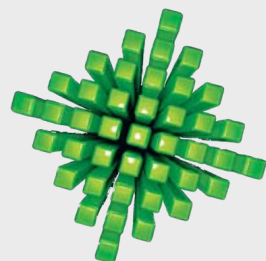


FIGURE 6.37 Increase in the width of a strip (spreading) during flat rolling. Spreading can be similarly observed when dough is rolled on a flat surface with a rolling pin.



Defects in Rolling

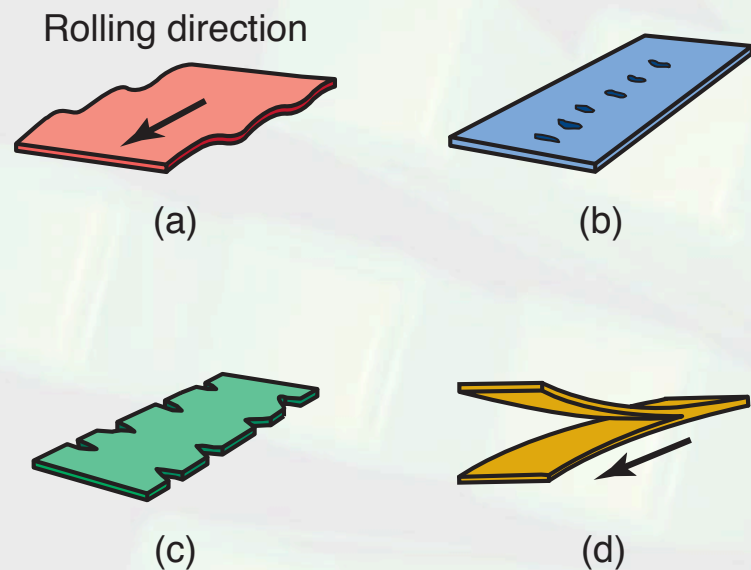


FIGURE 6.38 Schematic illustration of some defects in flat rolling: (a) wavy edges; (b) zipper cracks in the center of strip; (c) edge cracks; (d) alligating.

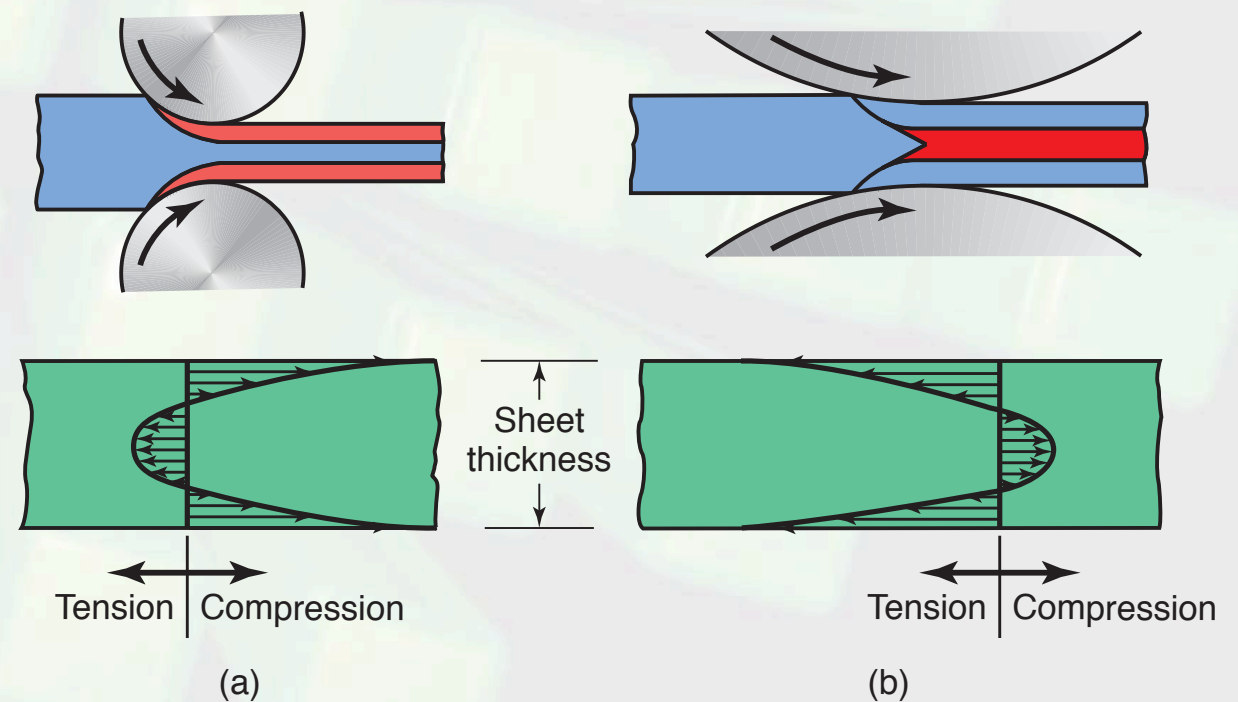
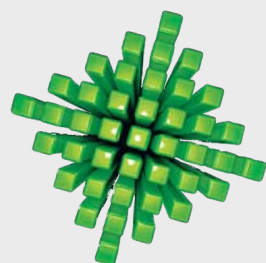


FIGURE 6.39 The effect of roll radius on the type of residual stresses developed in flat rolling: (a) small rolls and/or small reduction in thickness; and (b) large rolls and/or large reduction in thickness.



Roller Leveling

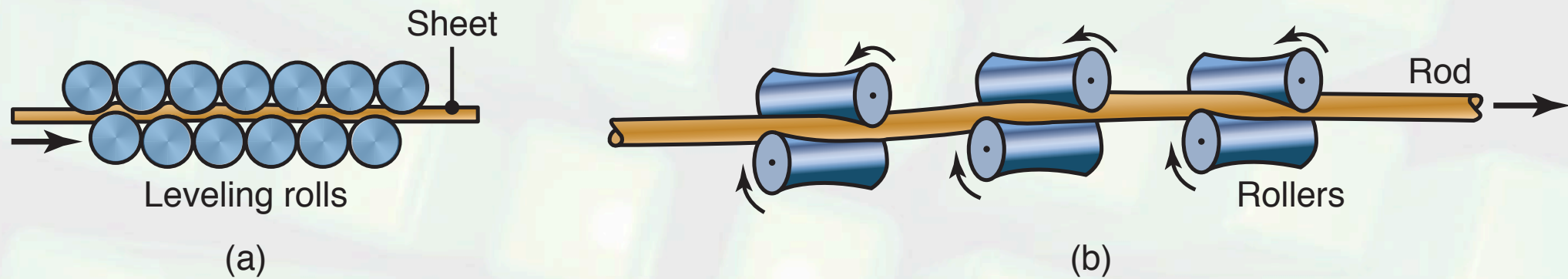
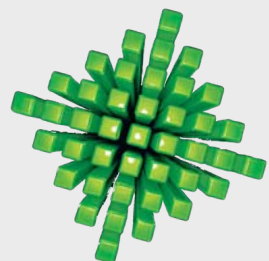


FIGURE 6.40 Schematic illustrations of roller leveling to (a) flatten rolled sheets and (b) straighten round rods.



Roll Arrangements

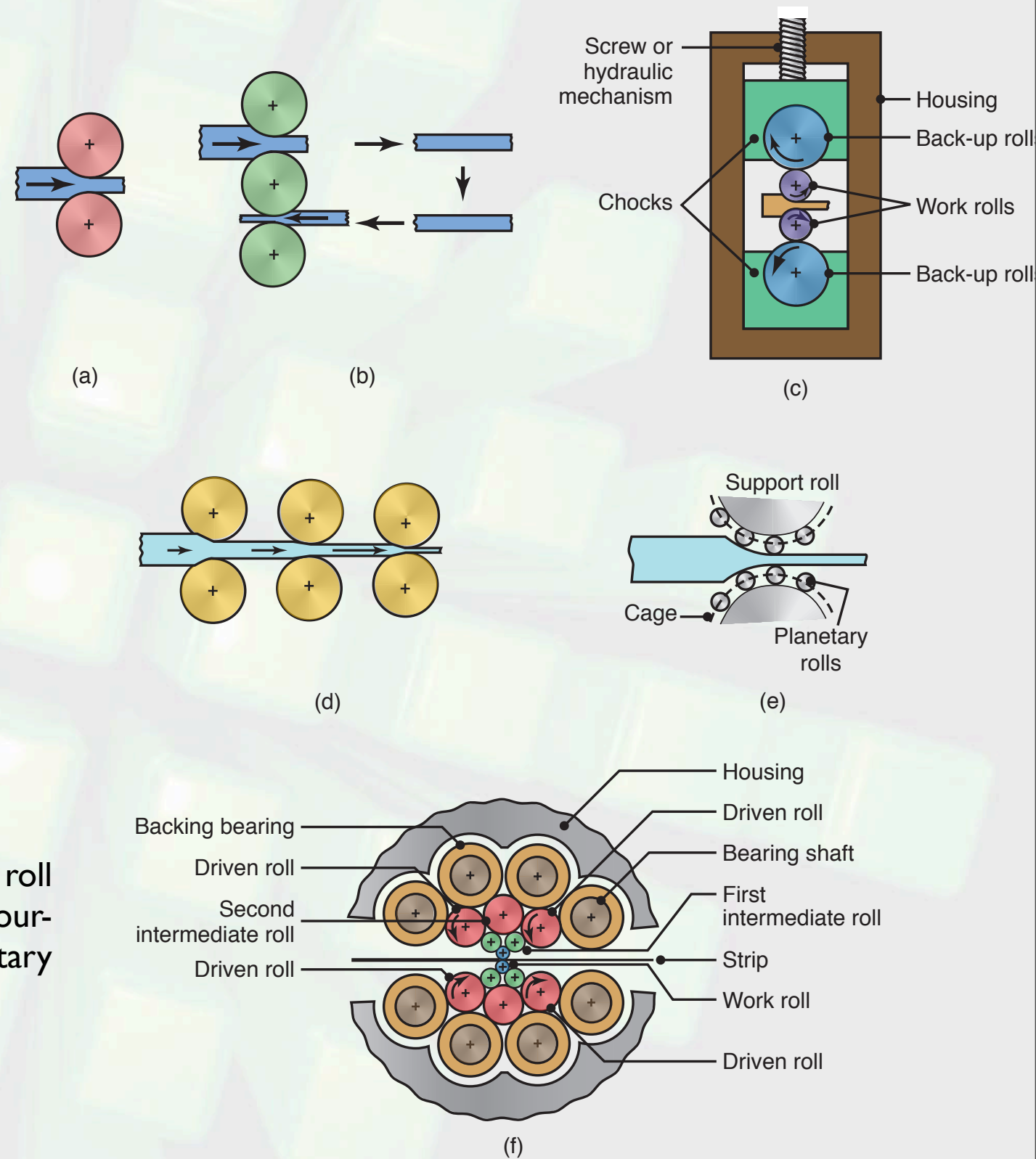
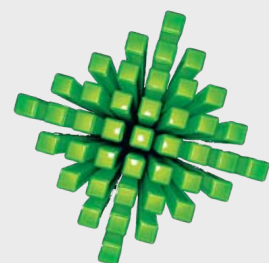


FIGURE 6.41 Schematic illustration of various roll arrangements: (a) two-high mill; (b) three-high mill; (c) four-high mill; (d) tandem rolling, with three stands; (e) planetary mill, (f) cluster (Sendzimir) mill.



Shape Rolling

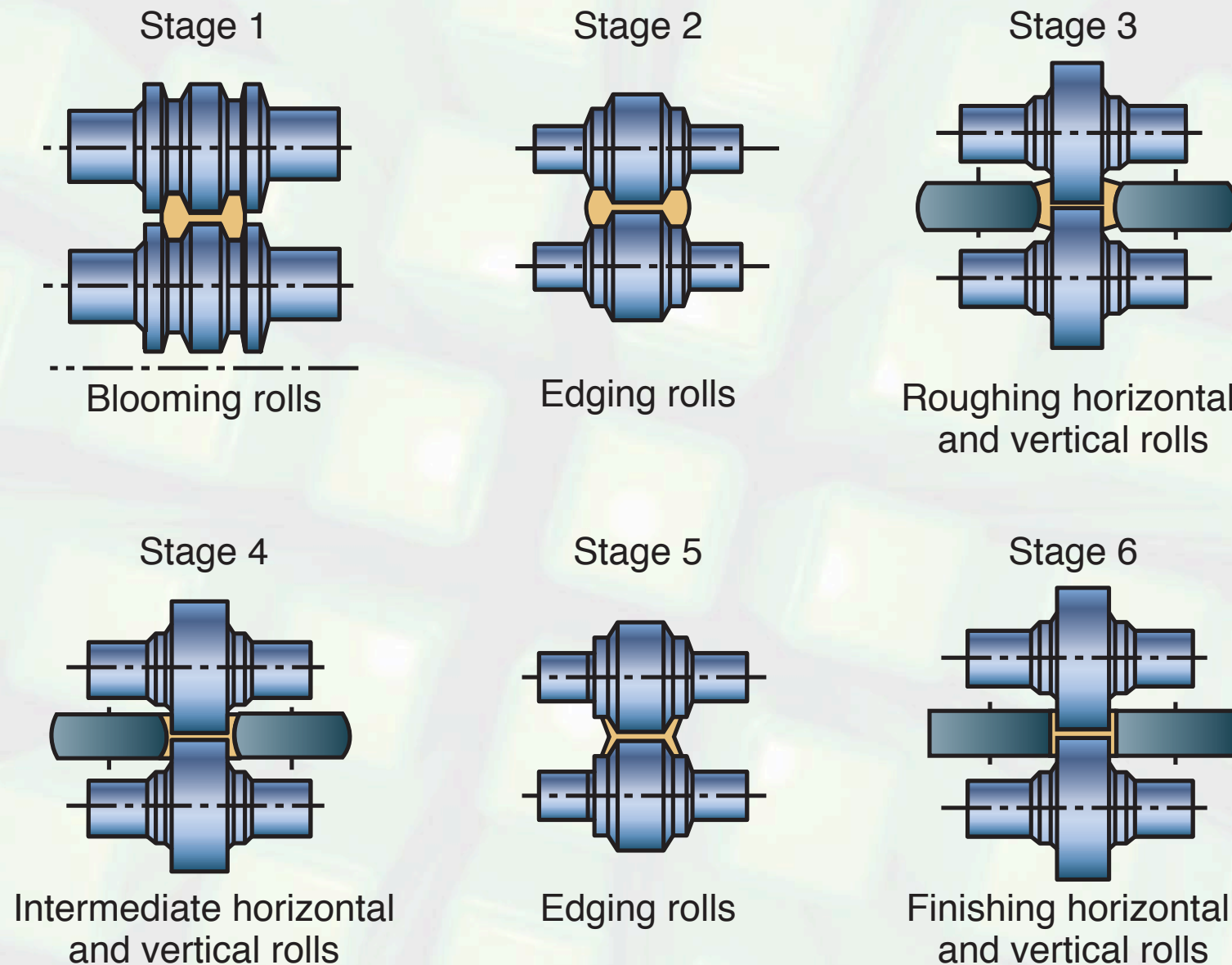
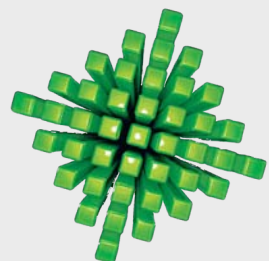


FIGURE 6.42 Stages in shape rolling of an H-section. Several other structural sections, such as channels and rails, also are rolled by this process.



Ring Rolling

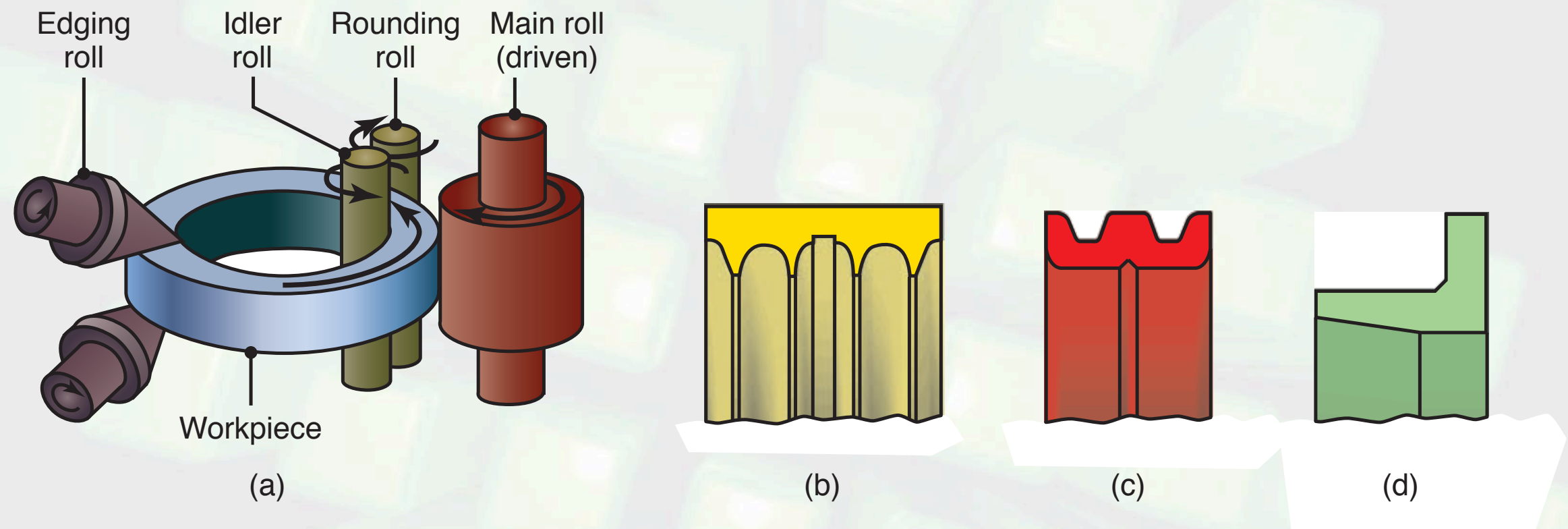
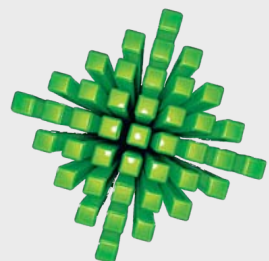
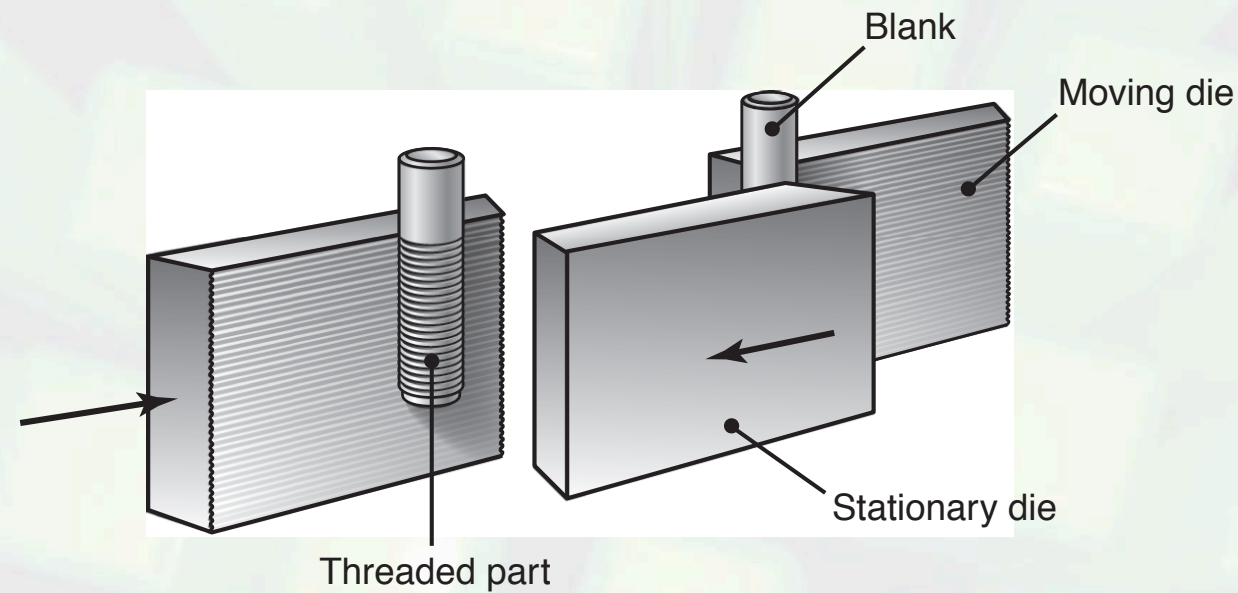


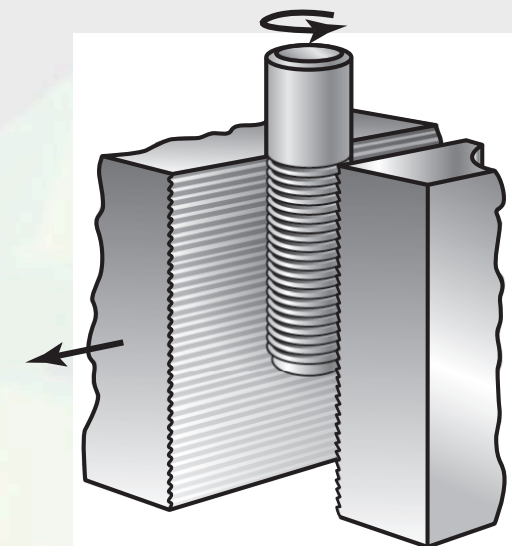
FIGURE 6.43 (a) Schematic illustration of a ring-rolling operation. Reducing the ring thickness results in an increase in its diameter. (b)-(d) Three examples of cross-sections that can be produced by ring rolling.



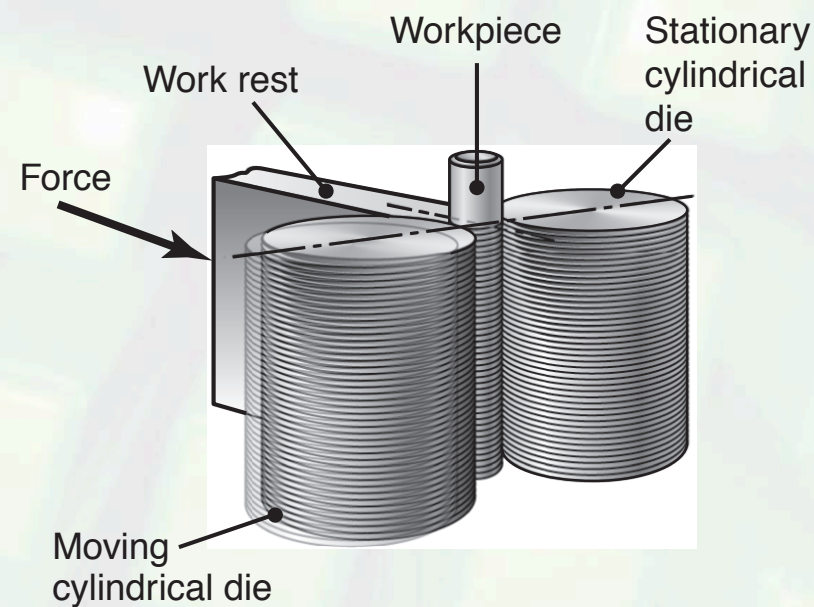
Thread Rolling



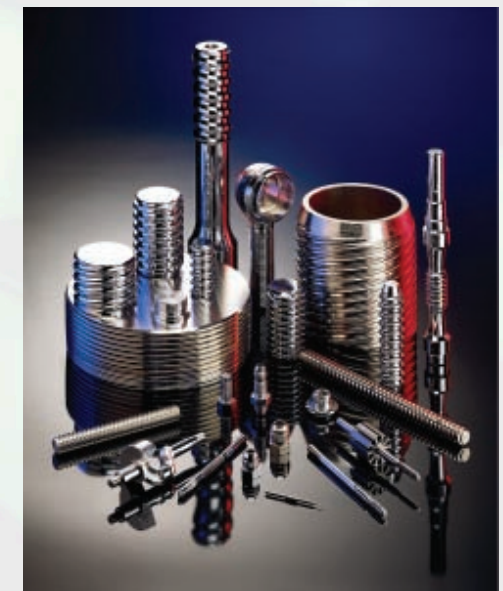
(a)



(b)

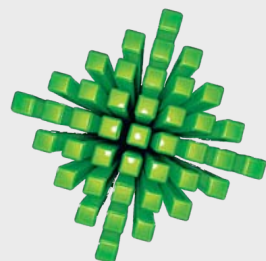


(c)



(d)

FIGURE 6.44 Thread-rolling processes: (a) and (b) reciprocating flat dies and (c) two-roller dies; (d) thread-rolled parts, made economically and at high production rates. *Source:* (d) Courtesy of Tesker Manufacturing Corp.



Thread Microstructure

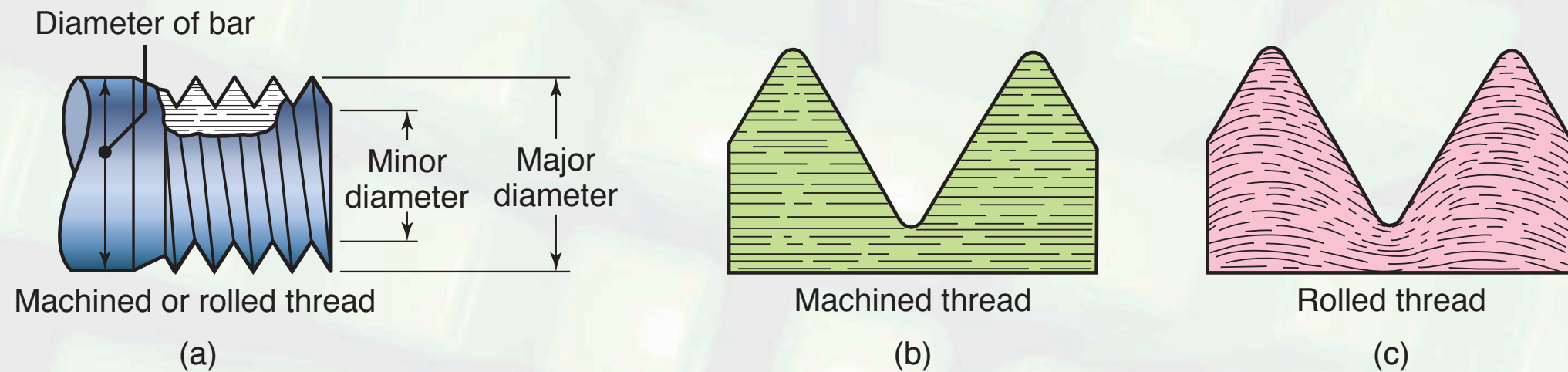
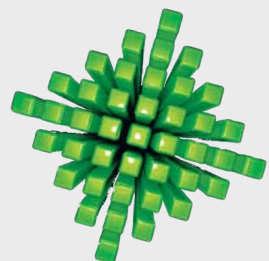


FIGURE 6.45 (a) Schematic illustration of thread features; (b) grain-flow lines in machined and (c) rolled threads. Note that unlike machined threads, which are cut through the grains of the metal, rolled threads follow the grains and because of the cold working involved, they are stronger.



Mannesmann Process

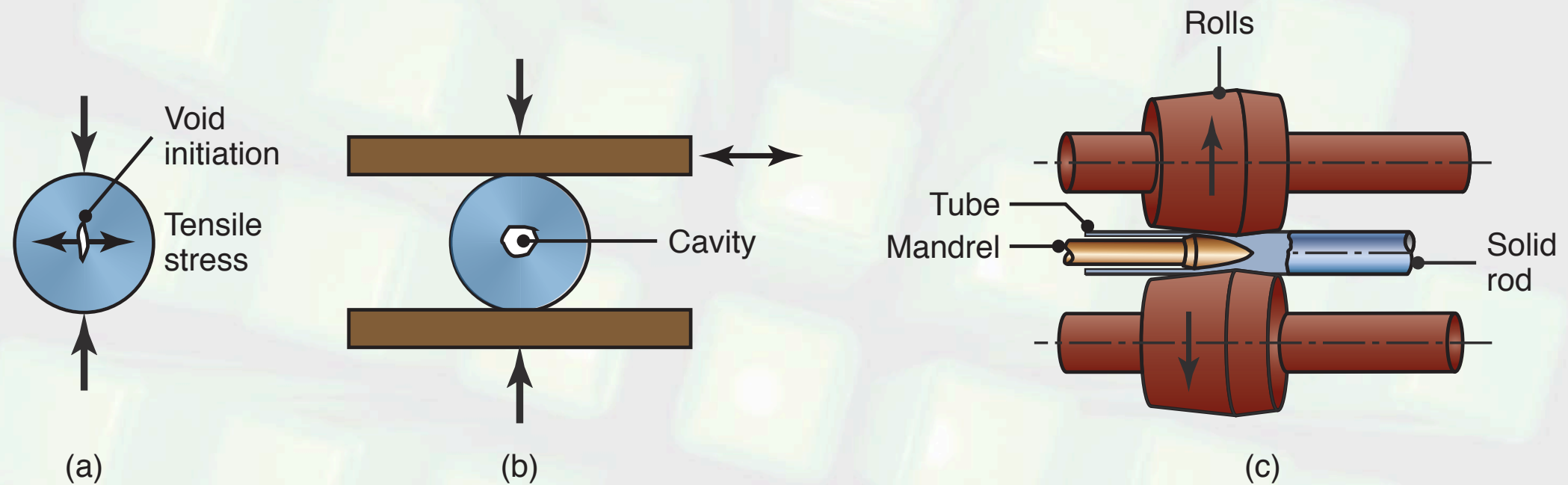
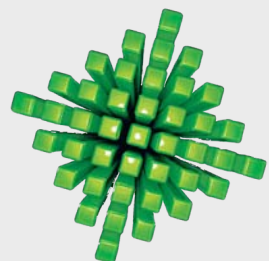
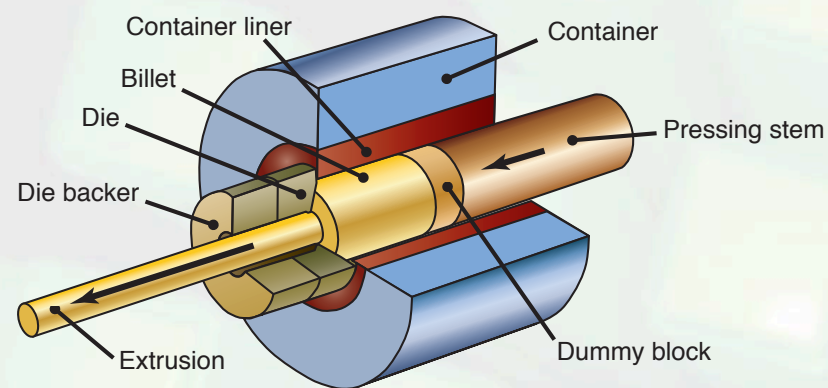


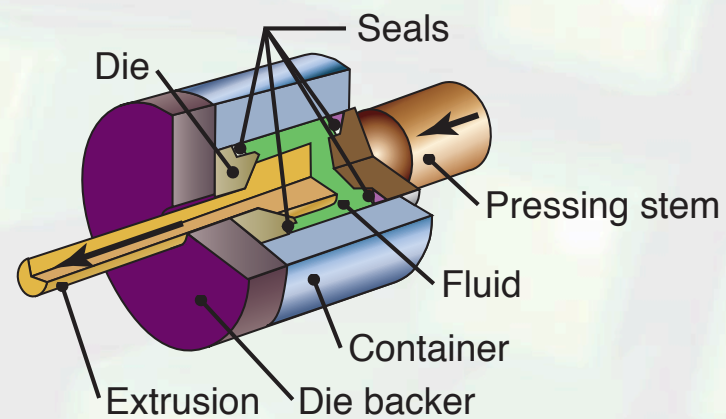
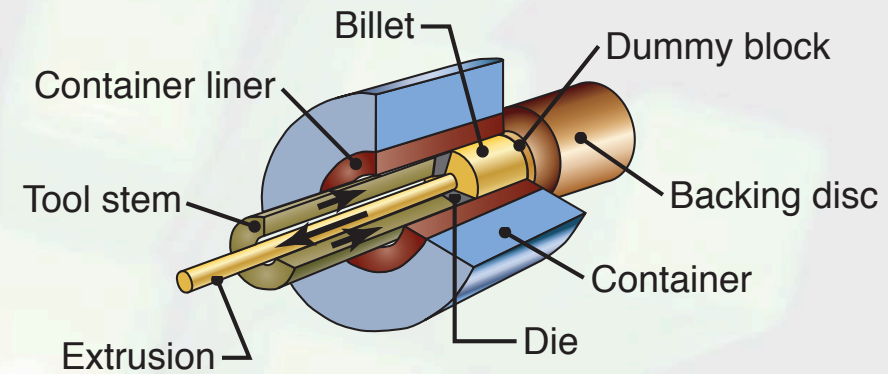
FIGURE 6.46 (a) Cracks developed in a solid round bar due to secondary tensile stresses; (b) simulation of the rotary-tube-piercing process; and (c) the Mannesmann process (mill) for seamless tube making. The mandrel is held in place by a long rod, although techniques also have been developed whereby the mandrel remains in place without using a rod.



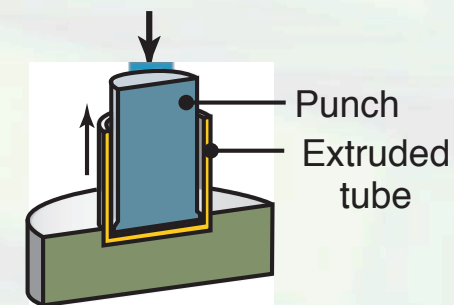
Types of Extrusion



(a)

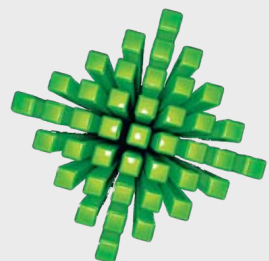


(c)

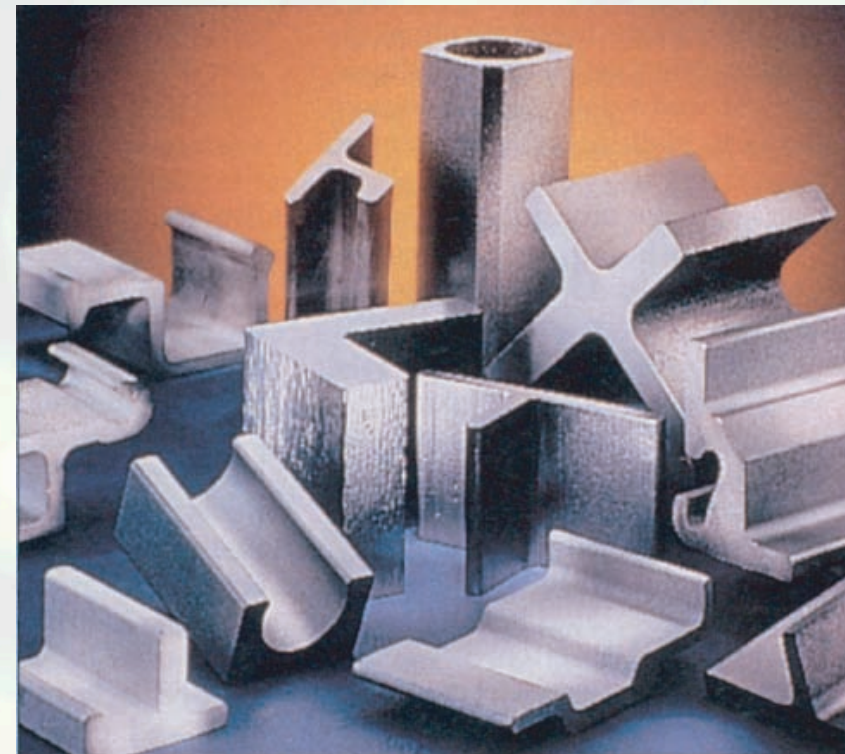
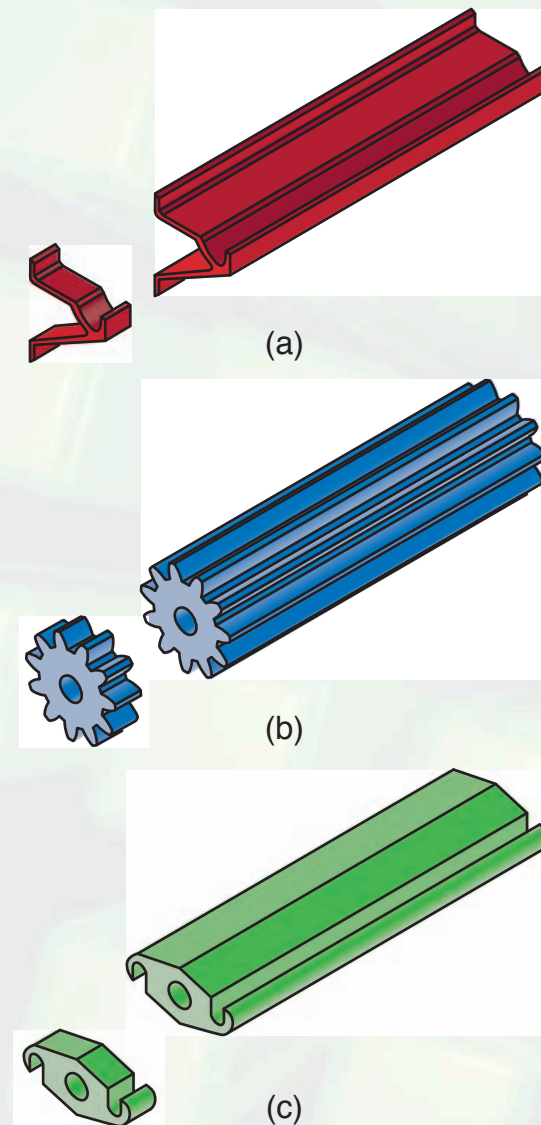


(d)

FIGURE 6.47 Types of extrusion: (a) direct; (b) indirect; (c) hydrostatic; (d) impact.

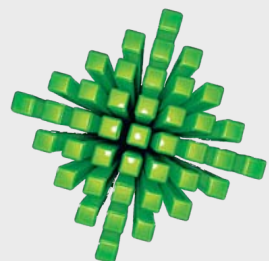


Extruded Products

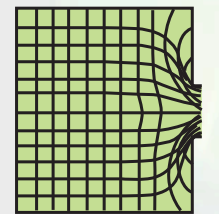


(d)

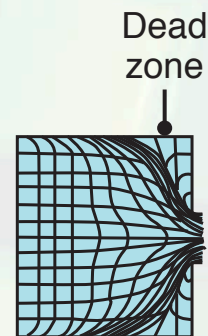
FIGURE 6.48 (a)-(c) Examples of extrusions and products made by sectioning them. *Source:* Kaiser Aluminum. (d) Examples of extruded cross-sections. *Source:* (d) Courtesy of Plymouth Extruded Shapes.



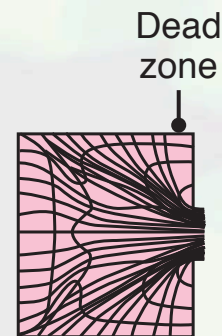
Metal Flow in Extrusion



(a)



(b)



(c)

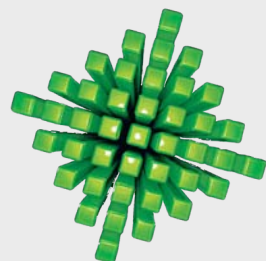
Slab method prediction for extrusion pressure:

$$p = Y \left(1 + \frac{\tan \alpha}{\mu} \right) [R^{\mu \cot \alpha} - 1]$$

Extrusion pressure with 45° dead-metal zone:

$$p = Y \left(1.7 \ln R + \frac{2L}{D_o} \right)$$

FIGURE 6.49 Schematic illustration of three different types of metal flow in direct extrusion. The die angle in these illustrations is 90°.



Mechanics of Extrusion

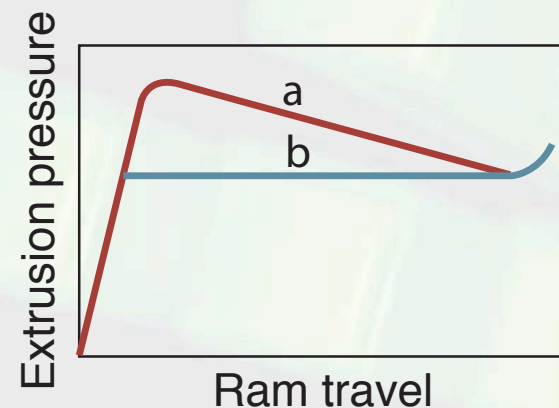


FIGURE 6.50 Schematic illustration of typical extrusion pressure as a function of ram travel: (a) direct extrusion and (b) indirect extrusion. The pressure in direct extrusion is higher because of frictional resistance at the container-billet interfaces, which decreases as the billet length decreases in the container.

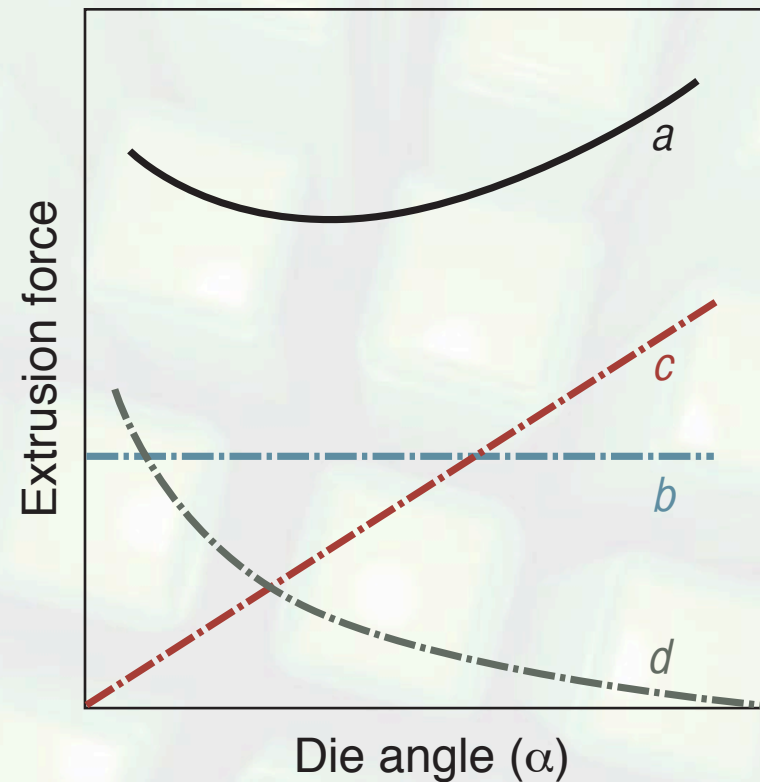


FIGURE 6.51 Schematic illustration of extrusion force as a function of die angle: (a) total force; (b) ideal force; (c) force required for redundant deformation; (d) force required to overcome friction. Note that there is a die angle where the total extrusion force is a minimum (optimum die angle).

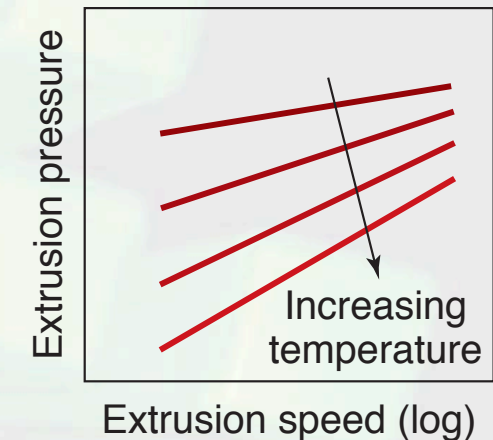
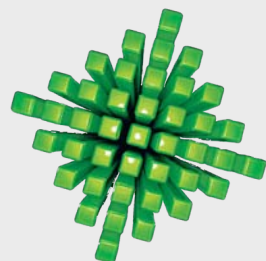
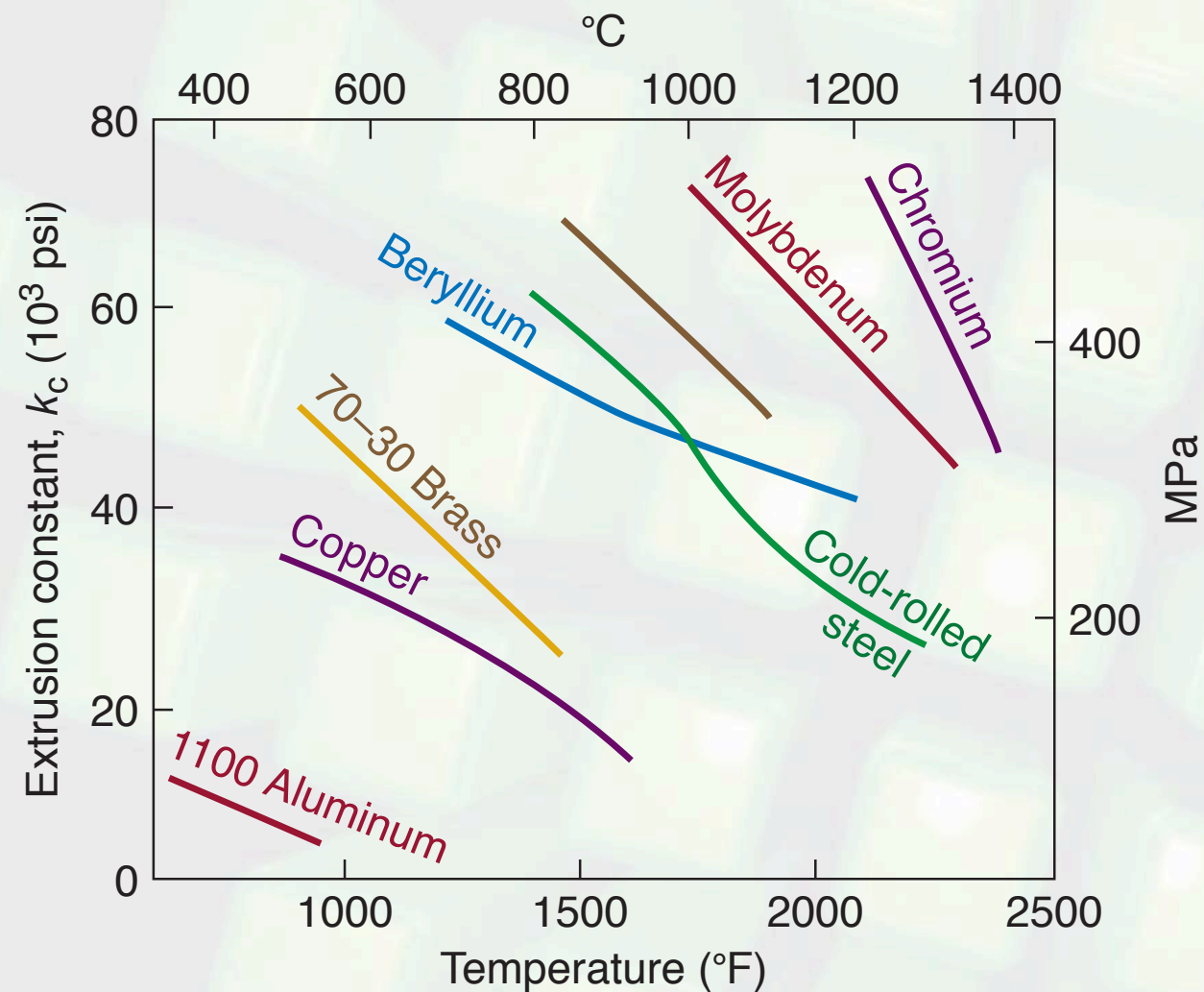


FIGURE 6.52 Schematic illustration of the effect of temperature and ram speed on extrusion pressure. Note the similarity of this figure with Fig. 2.10.

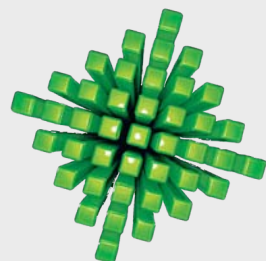


Extrusion Constant



$$p = K_e \ln R$$

FIGURE 6.51 Extrusion constant, K_e , for various materials as a function of temperature. Source: After P. Loewenstein.



Cold Extrusion

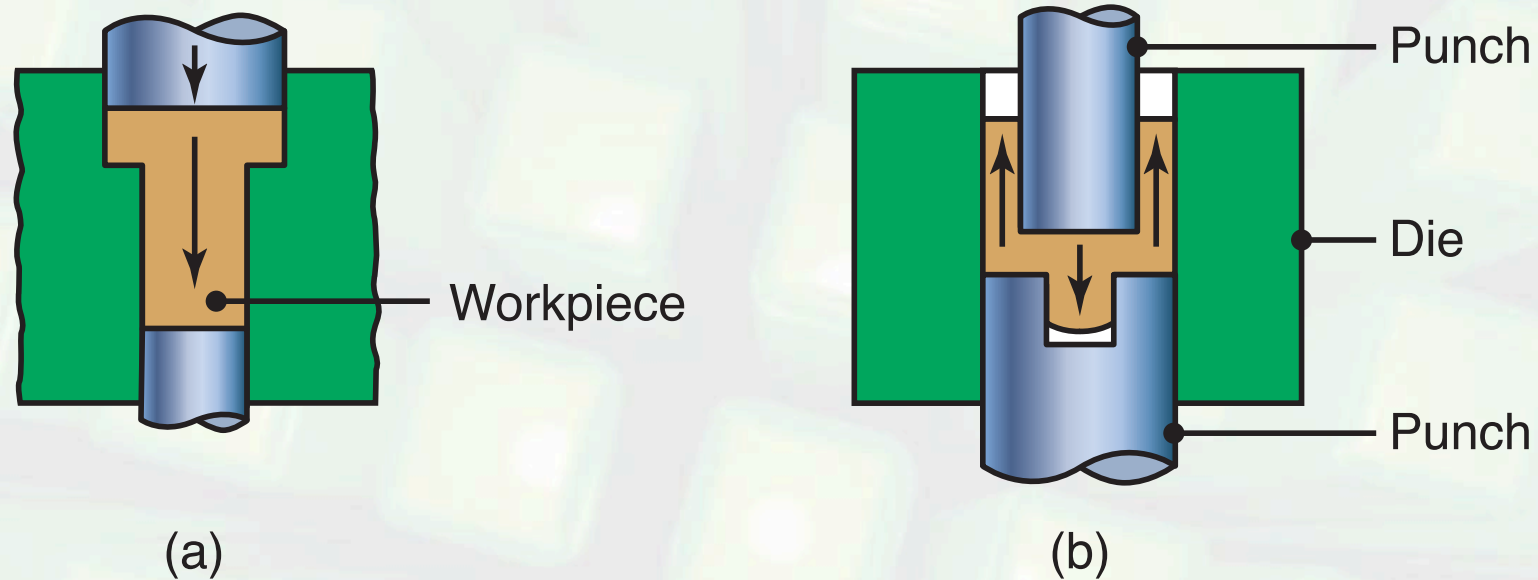
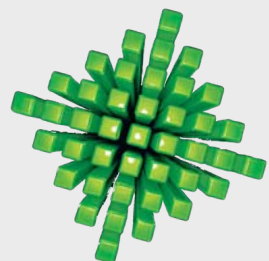


FIGURE 6.54 Two examples of cold extrusion. Arrows indicate the direction of material flow. These parts may also be considered as forgings.



Impact Extrusion

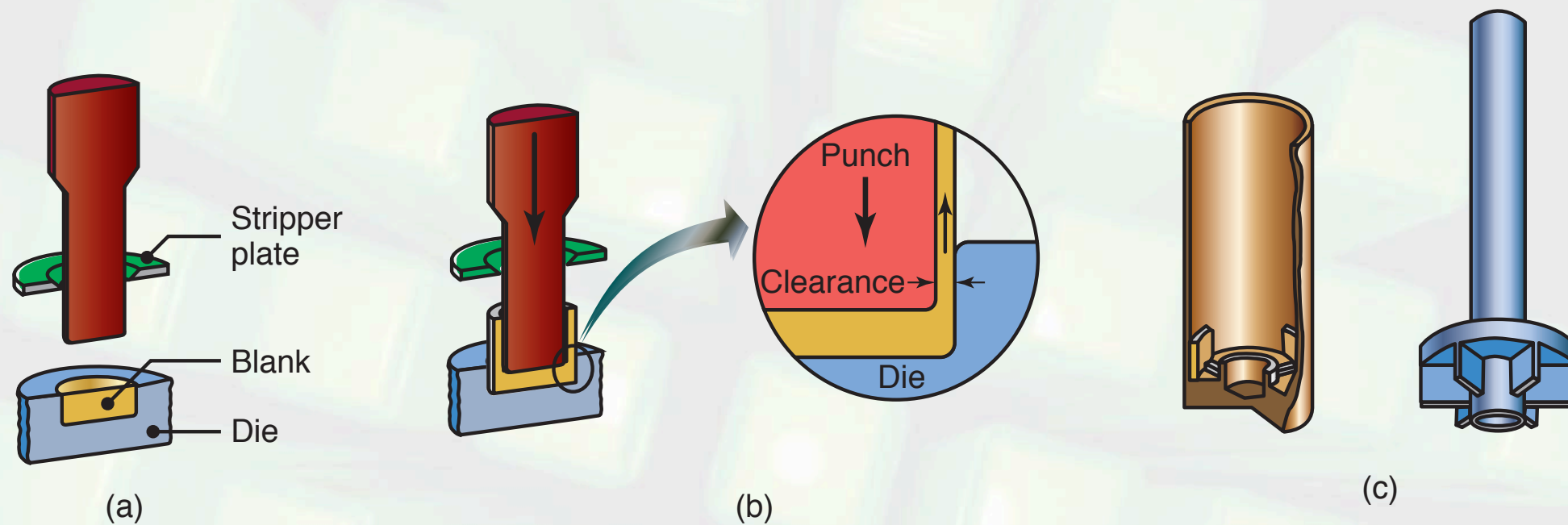
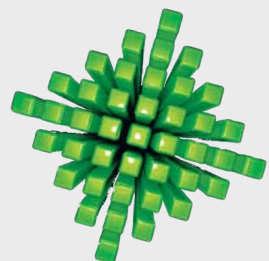


FIGURE 6.55 (a)-(b) Schematic illustration of the impact-extrusion process. The extruded parts are stripped using a stripper plate, as otherwise they may stick to the punch. (c) Two examples of products made by impact extrusion. Collapsible tubes can be produced by impact extrusion, referred to as the Hooker process.



Extrusion Pressure

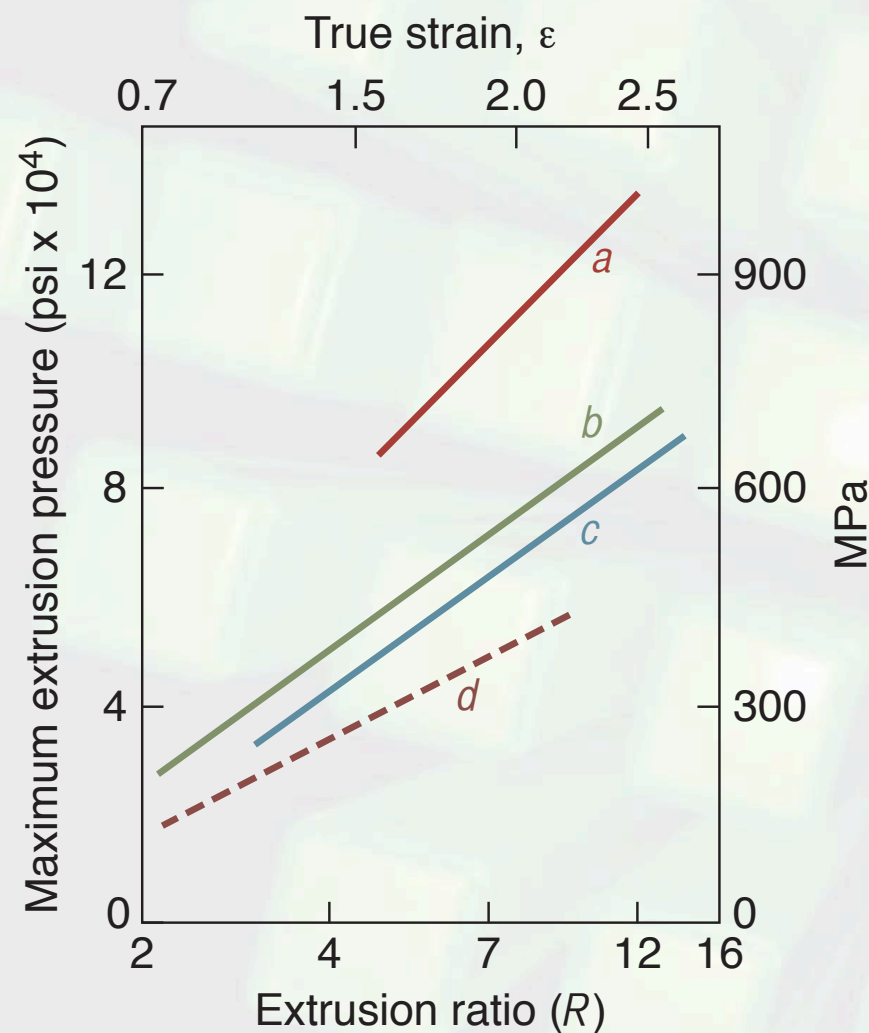
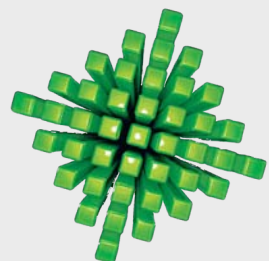
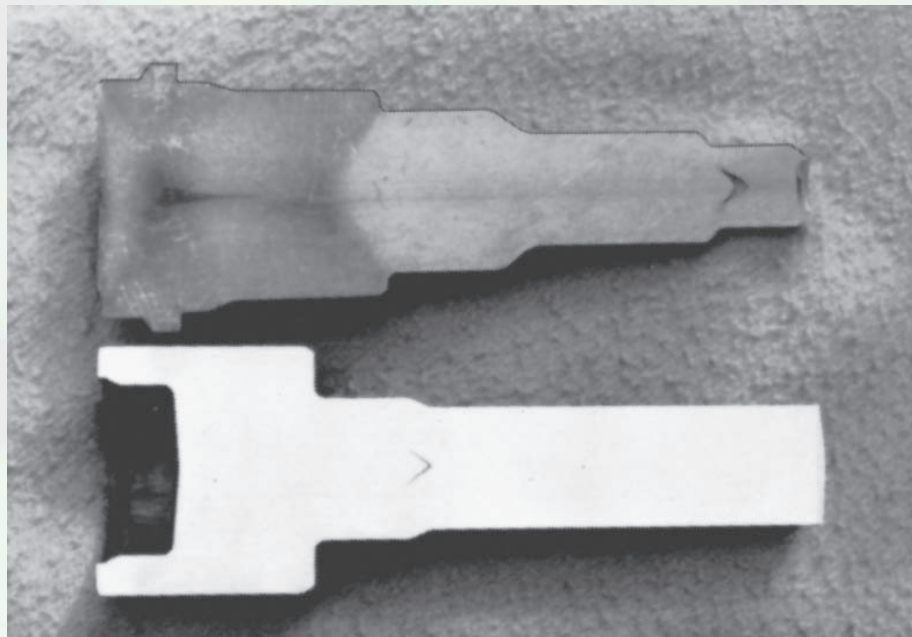


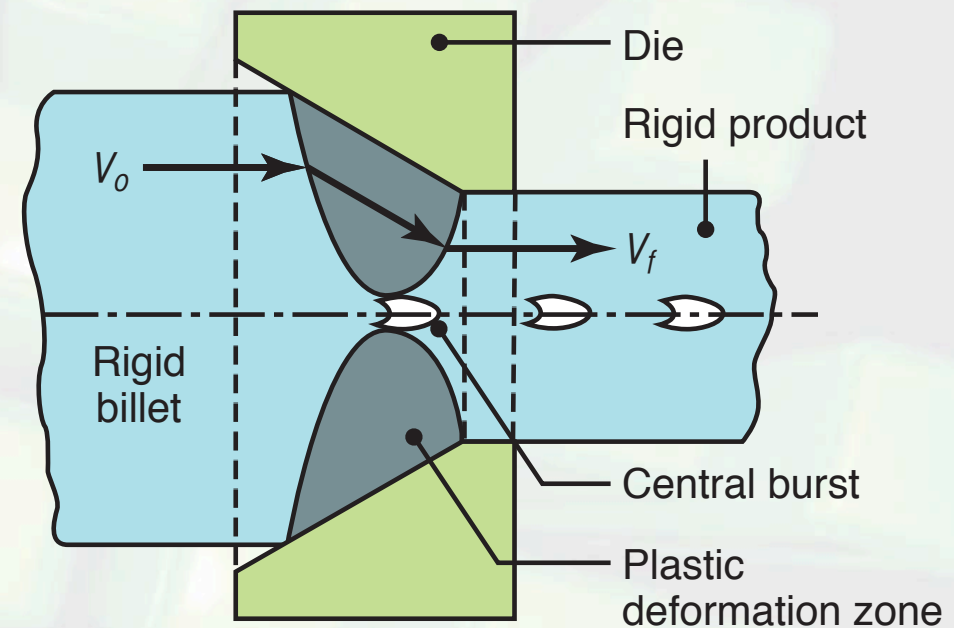
FIGURE 6.56 Extrusion pressure as a function of the extrusion ratio for an aluminum alloy. (a) Direct extrusion, $\alpha = 90^\circ$. (b) Hydrostatic extrusion, $\alpha = 45^\circ$. (c) Hydrostatic extrusion, $\alpha = 22.5^\circ$. (d) Ideal homogeneous deformation, calculated. Source: After H. Li, D. Pugh, and K. Ashcroft.



Chevron Cracking Defect

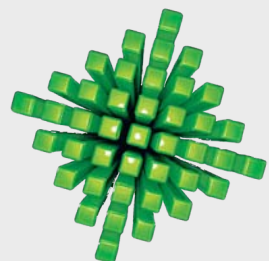


(a)



(b)

FIGURE 6.57 a) Chevron cracking in round steel bars during extrusion. Unless the part is inspected, such internal defects may remain undetected and possibly cause failure of the part in service. (b) Deformation zone in extrusion, showing rigid and plastic zones. Note that the plastic zones do not meet, leading to chevron cracking. The same observations are also made in drawing round bars through conical dies and drawing flat sheet or plate through wedge-shaped dies. *Source: After B. Avitzur.*



Tube Extrusion

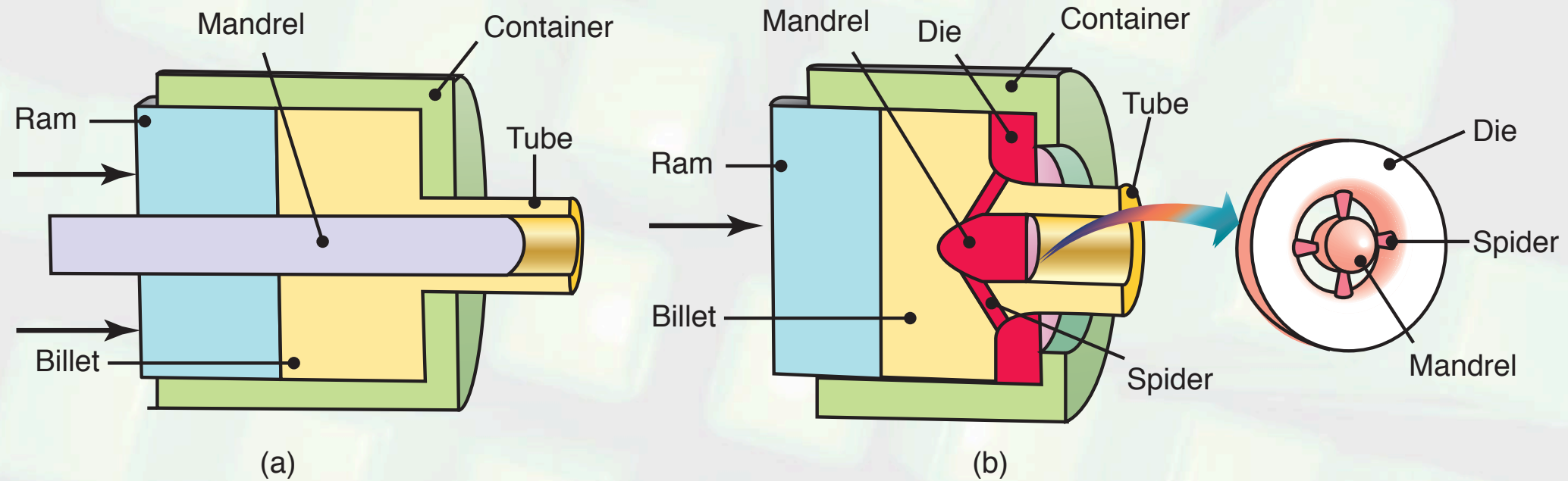
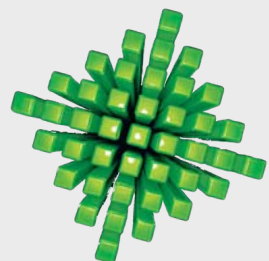


FIGURE 6.58 Extrusion of a seamless tube. (a) Using an internal mandrel that moves independently of the ram. An alternative arrangement has the mandrel integral with the ram. (b) Using a spider die (see Fig. 6.59c) to produce seamless tubing.



Extrusion of Hollow Shapes

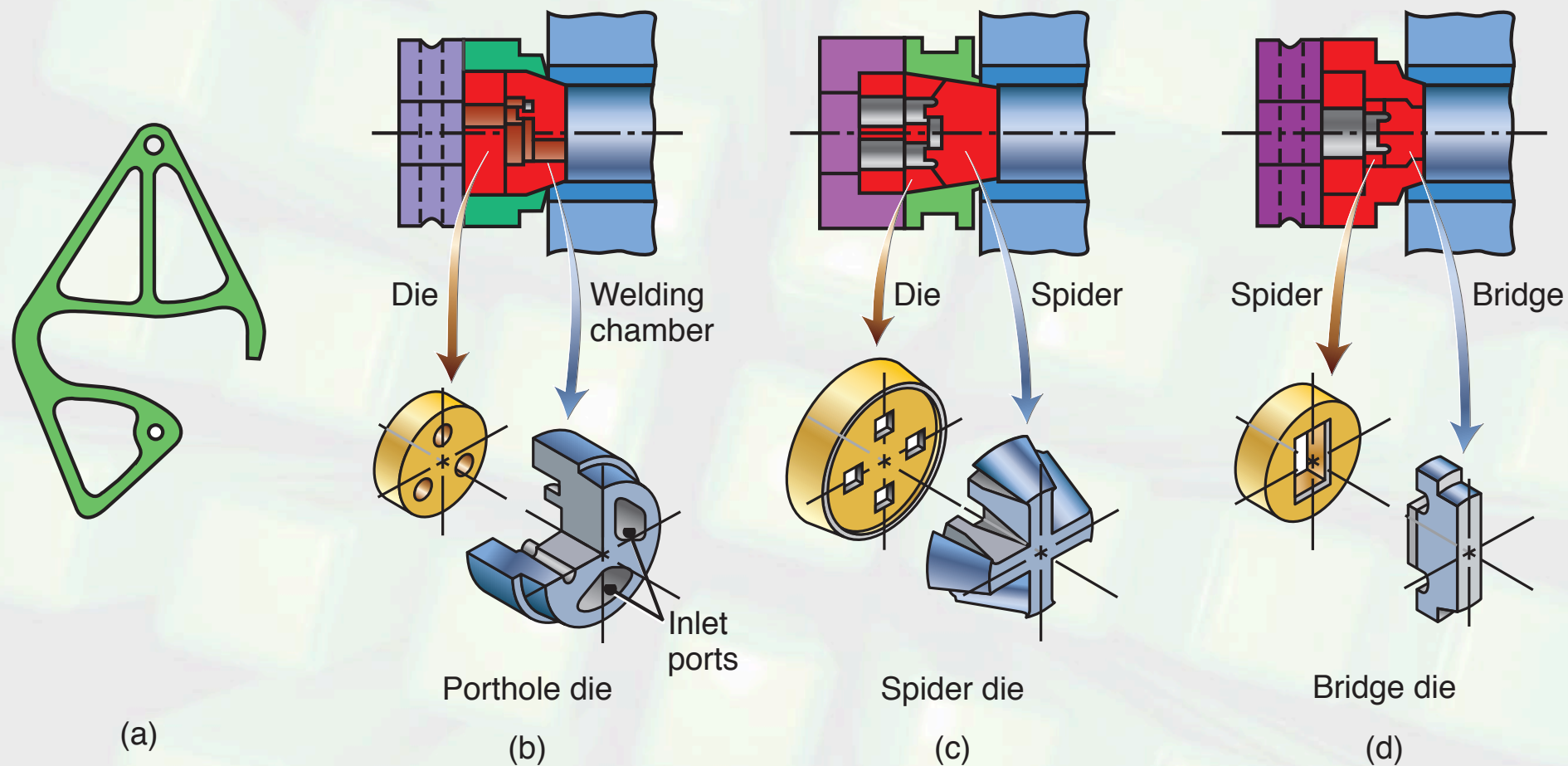
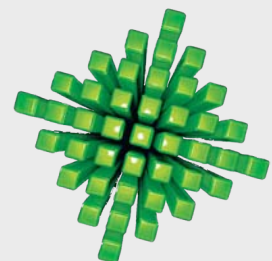


FIGURE 6.59 (a) An extruded 6063-T6 aluminum ladder lock for aluminum extension ladders. This part is 8 mm (5/16 in.) thick and is sawed from the extrusion, as also shown in Fig. 6.48a. (b)-(d) Components of various types of dies for extruding intricate hollow shapes. *Source:* After K. Laue and H. Stenger



Rod or Wire Drawing

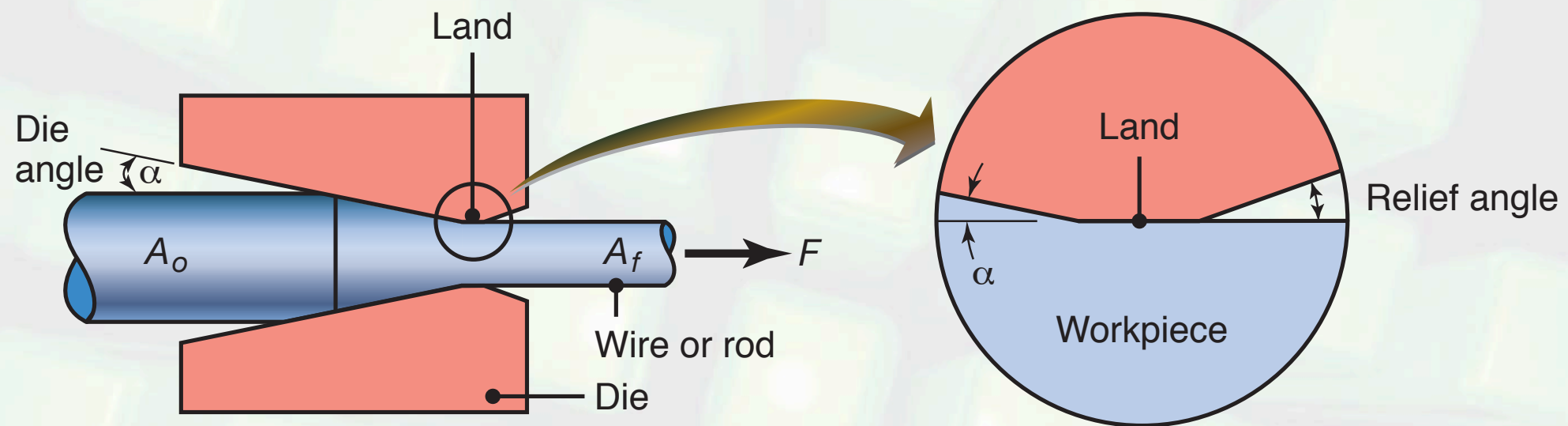
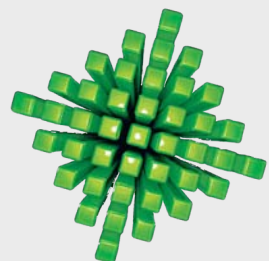
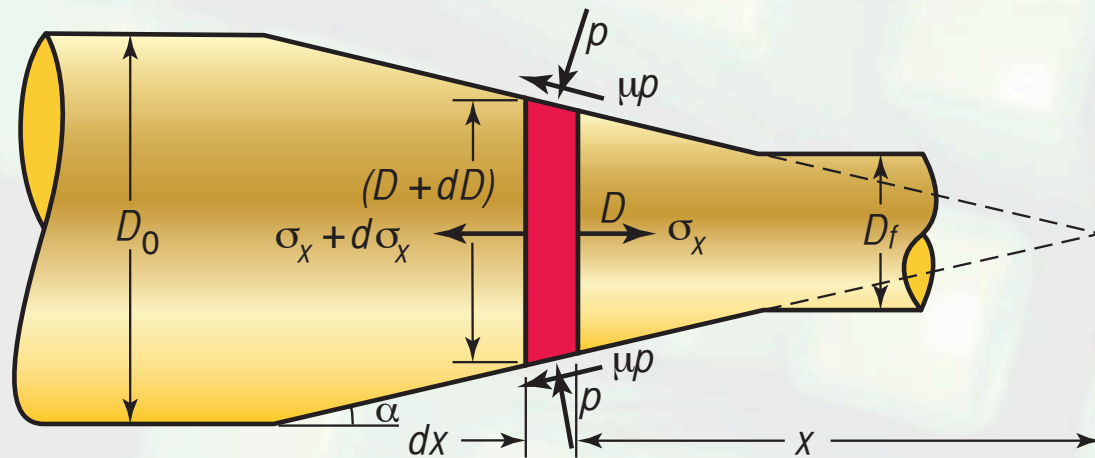


FIGURE 6.60 Variables in drawing round rod or wire.



Slab Analysis for Drawing



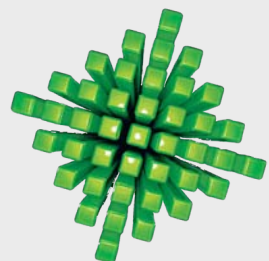
Drawing stress

$$\sigma_d = \Phi \bar{Y} \left(1 + \frac{\mu}{\alpha} \right) \ln \left(\frac{A_o}{A_f} \right)$$

Inhomogeneity factor

$$\Phi = 1 + 0.12 \left(\frac{h}{L} \right)$$

FIGURE 6.61 Stresses acting on an element in drawing of a solid cylindrical rod or wire through a converging conical die.



Drawing Stress

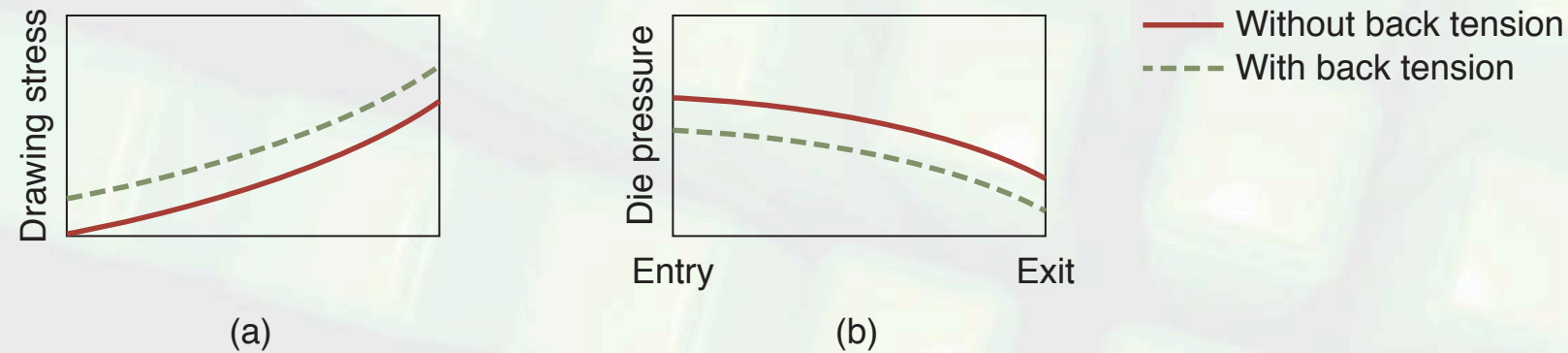


FIGURE 6.62 Variation in the (a) drawing stress and (b) die contact pressure along the deformation zone. Note that as the drawing stress increases, the die pressure decreases (see also yield criteria, described in Section 2.11). Note the effect of back tension on the stress and pressure.

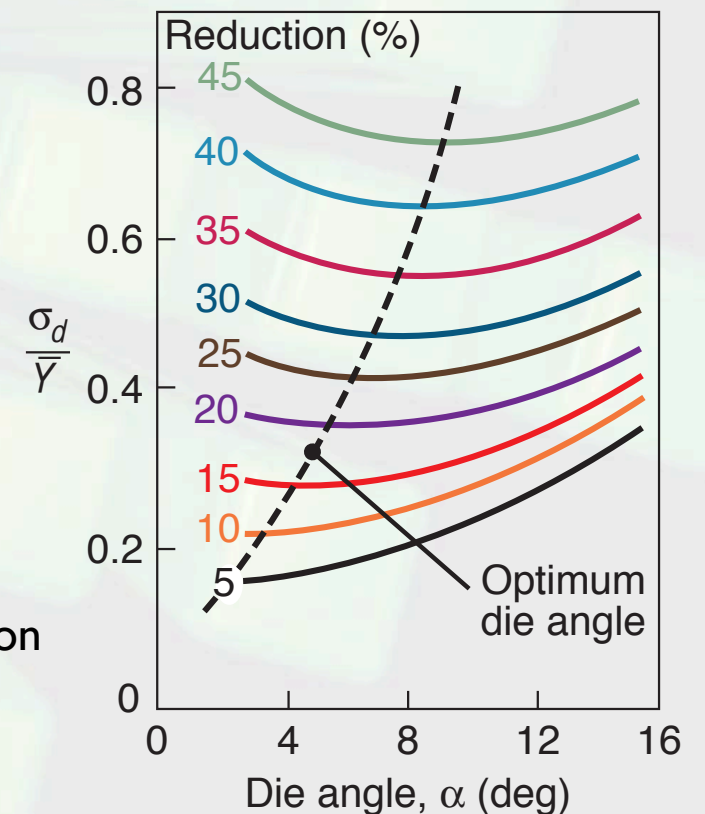
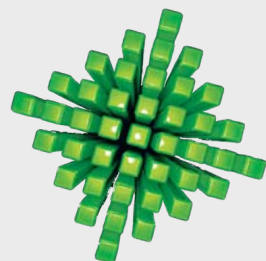


FIGURE 6.63 The effect of reduction in cross-sectional area on the optimum die angle in drawing. Source: After J.G. Wistreich.



Tube-Drawing Operations

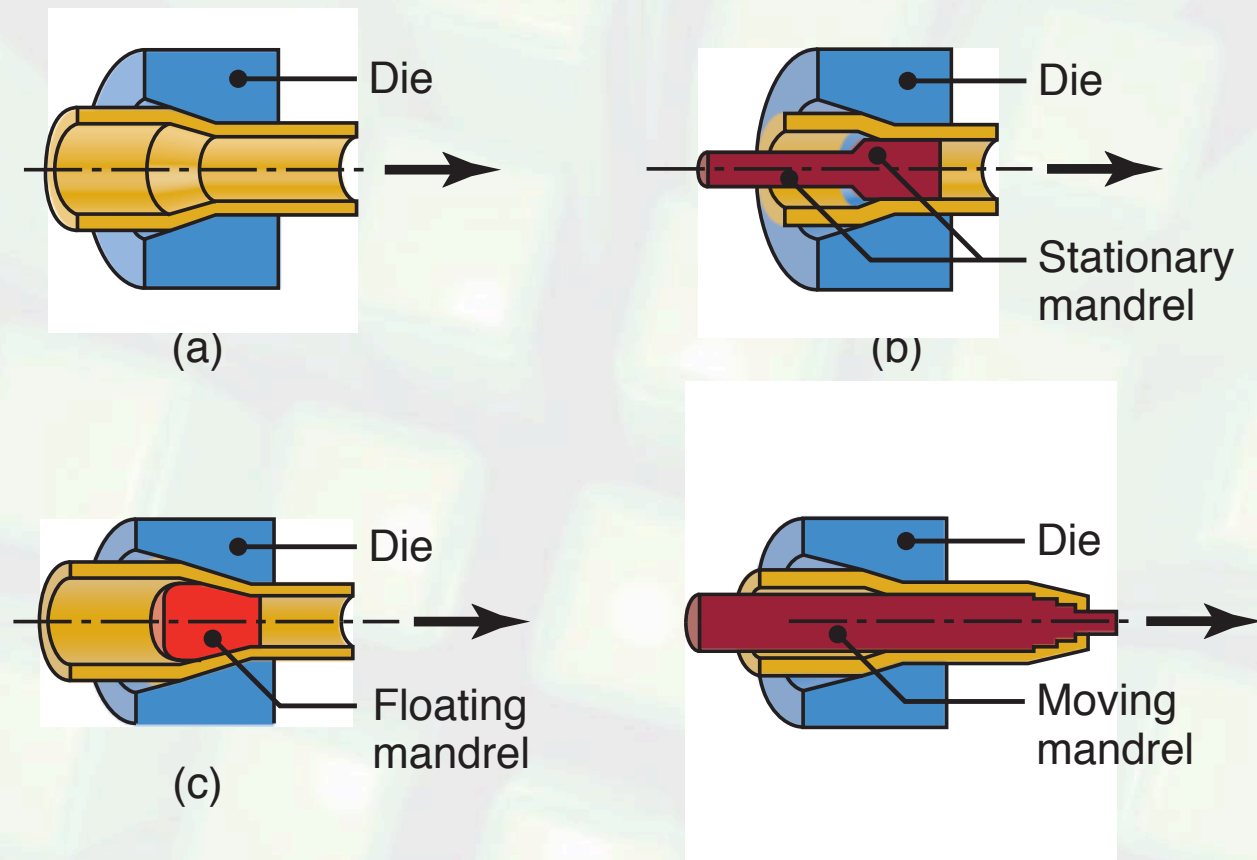
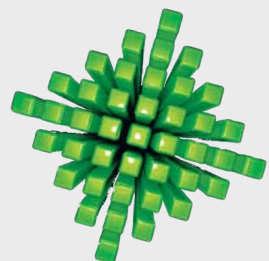


FIGURE 6.64 Examples of tube-drawing operations, with and without an internal mandrel. Note that a variety of diameters and wall thicknesses can be produced from the same tube stock (that has been produced by other processes, such as extrusion)



Residual Stresses in Drawing

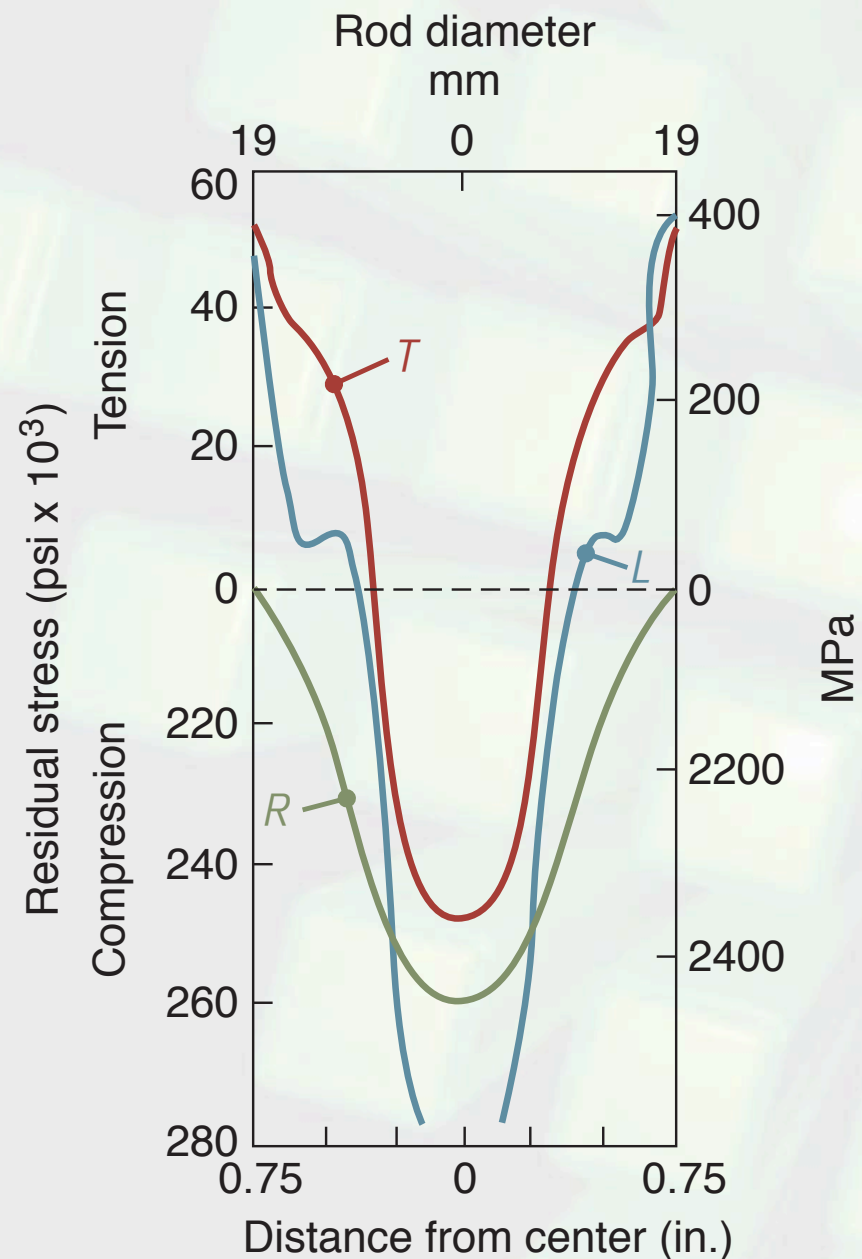
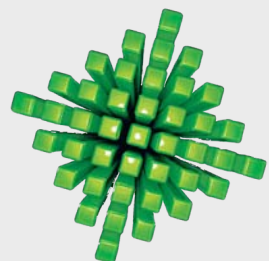


FIGURE 6.65 Residual stresses in cold-drawn 1045 carbon steel round rod: *T* = transverse direction, *L* = longitudinal direction and *R* = radial direction. Source: After E.S. Nachtman.



Drawing Dies

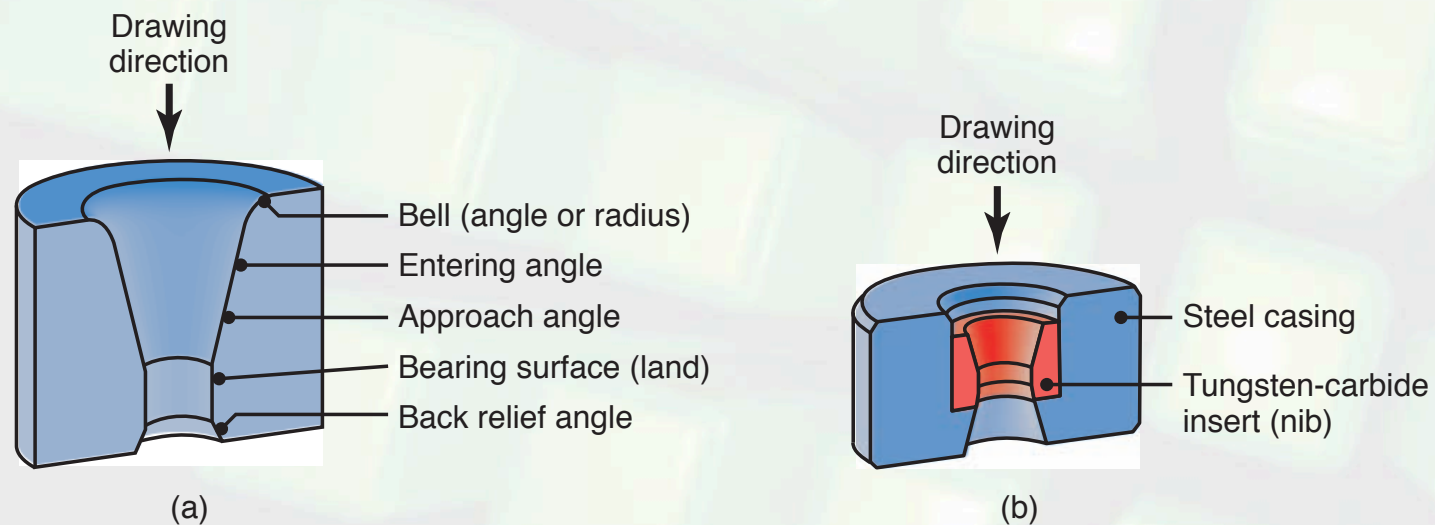


FIGURE 6.66 (a) Terminology for a typical die for drawing round rod or wire. (b) Tungsten-carbide die insert in a steel casing. Diamond dies, used in drawing thin wire, also are encased in a similar manner.

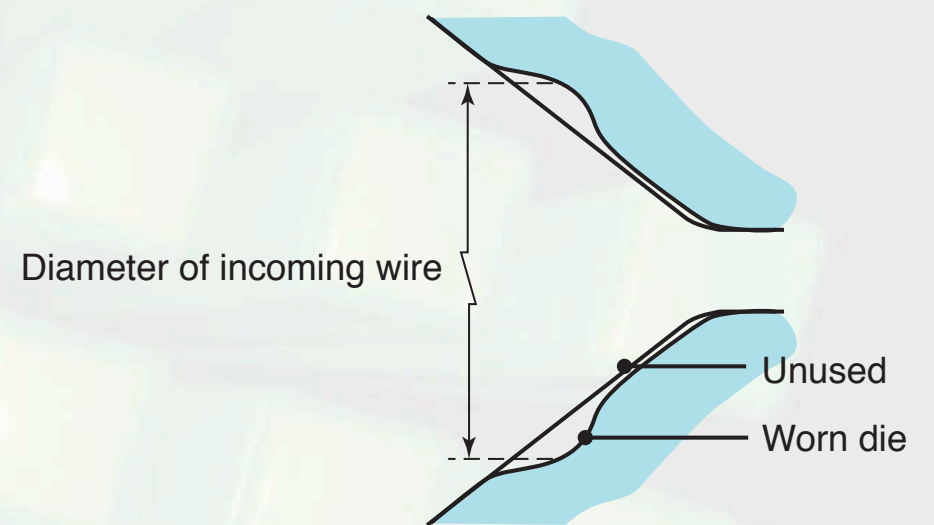
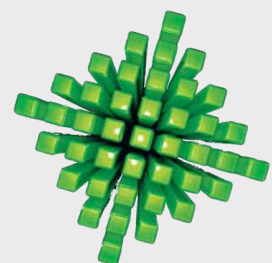


FIGURE 6.67 Schematic illustration of a typical wear pattern in a wire-drawing die.



Rotary Swaging

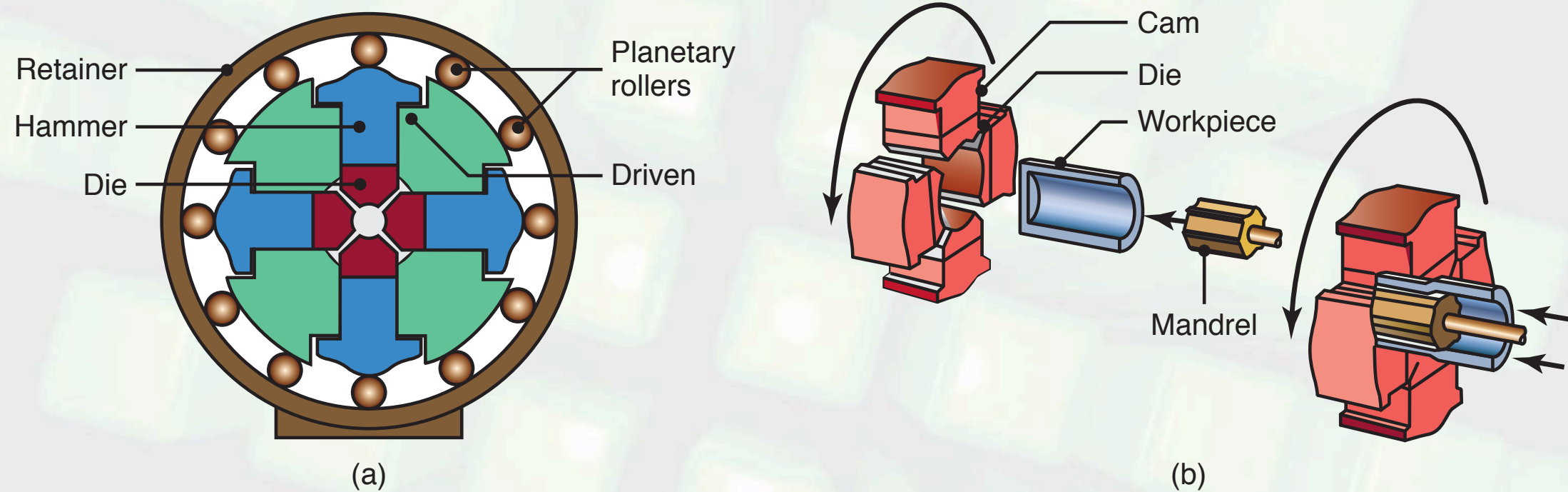
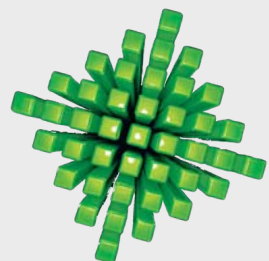


FIGURE 6.68 (a) Schematic illustration of the rotary-swaging process. (b) Forming internal profiles in a tubular workpiece by swaging.



Rotary Swaging

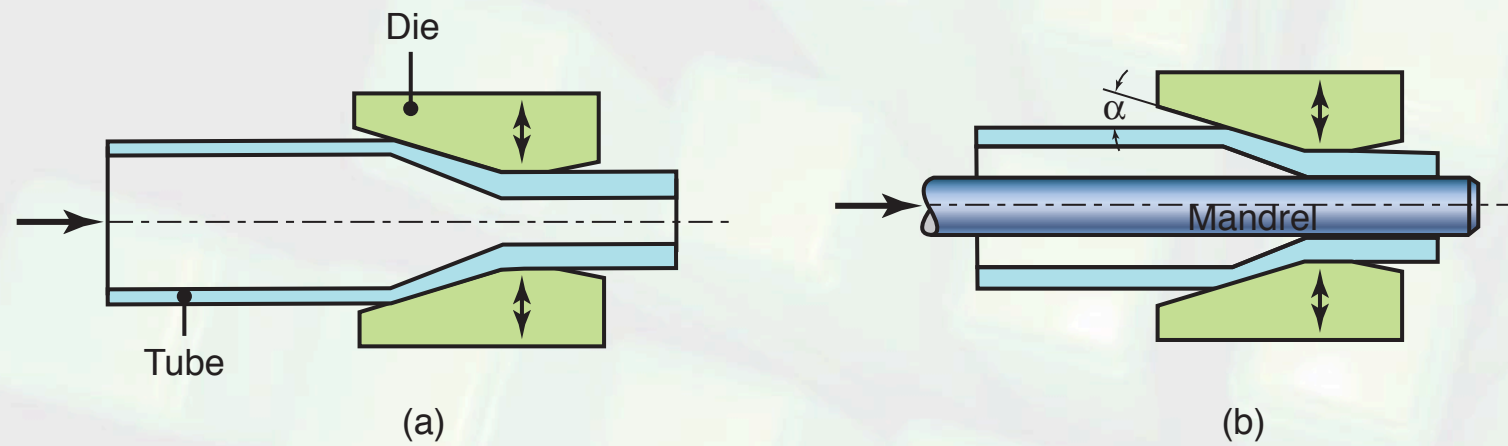
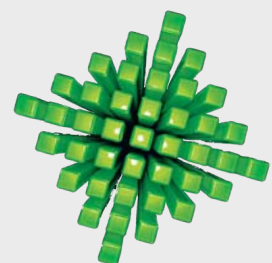
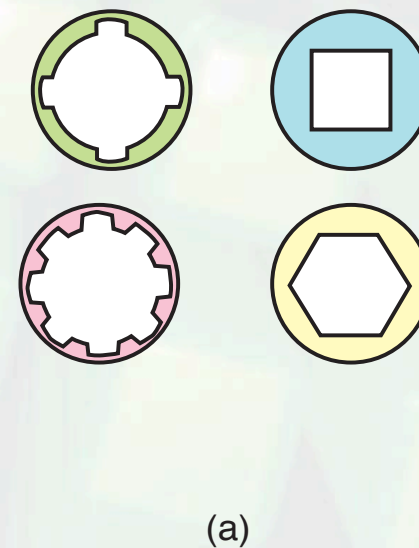


FIGURE 6.69 Reduction of outer and inner diameters of tubes by swaging. (a) Free sinking without a mandrel. The ends of solid bars and wire are tapered (pointing) by this process in order to feed the material into the conical die. (b) Sinking on a mandrel. Coaxial tubes of different materials can also be swaged in one operation.

FIGURE 6.70 (a) Typical cross-sections produced by swaging tubular blanks with a constant wall thickness on shaped mandrels. Rifling of small gun barrels also can be made by swaging. (b) Typical parts made by swaging. Source: Courtesy of J. Richard Industries.



Forming Economics

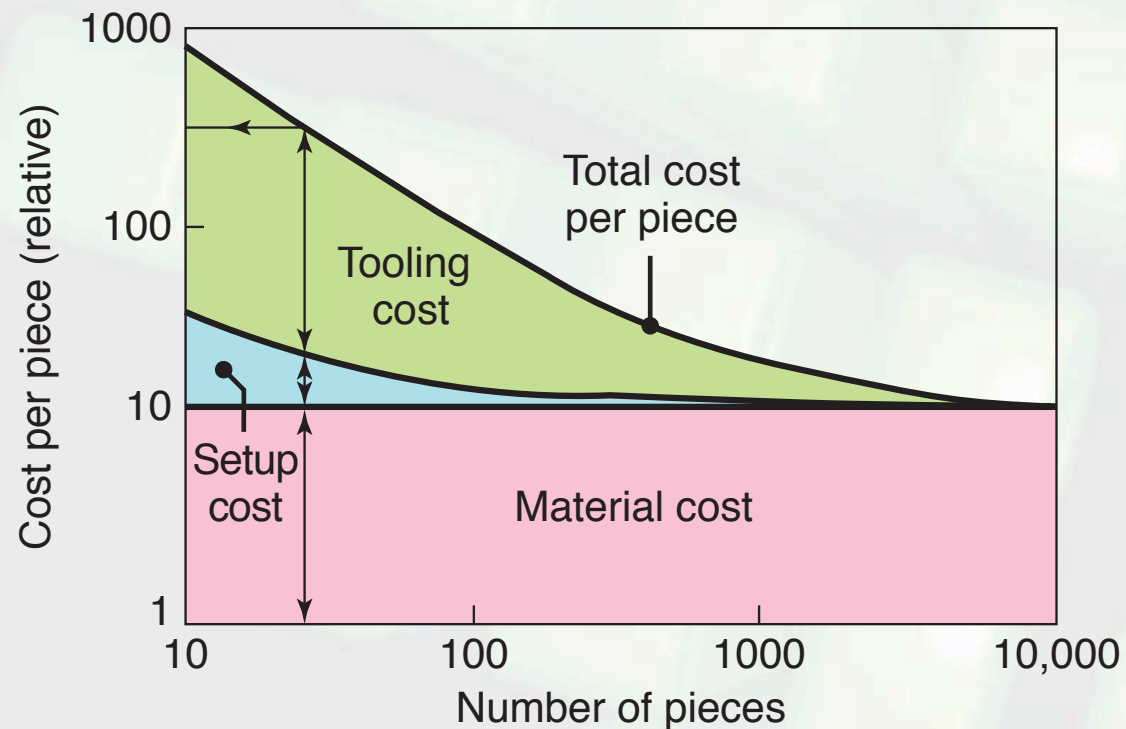


FIGURE 6.71 Typical unit cost (cost per piece) in forging. Note how the setup and the tooling costs per piece decrease as the number of pieces forged increases, if all pieces use the same die.

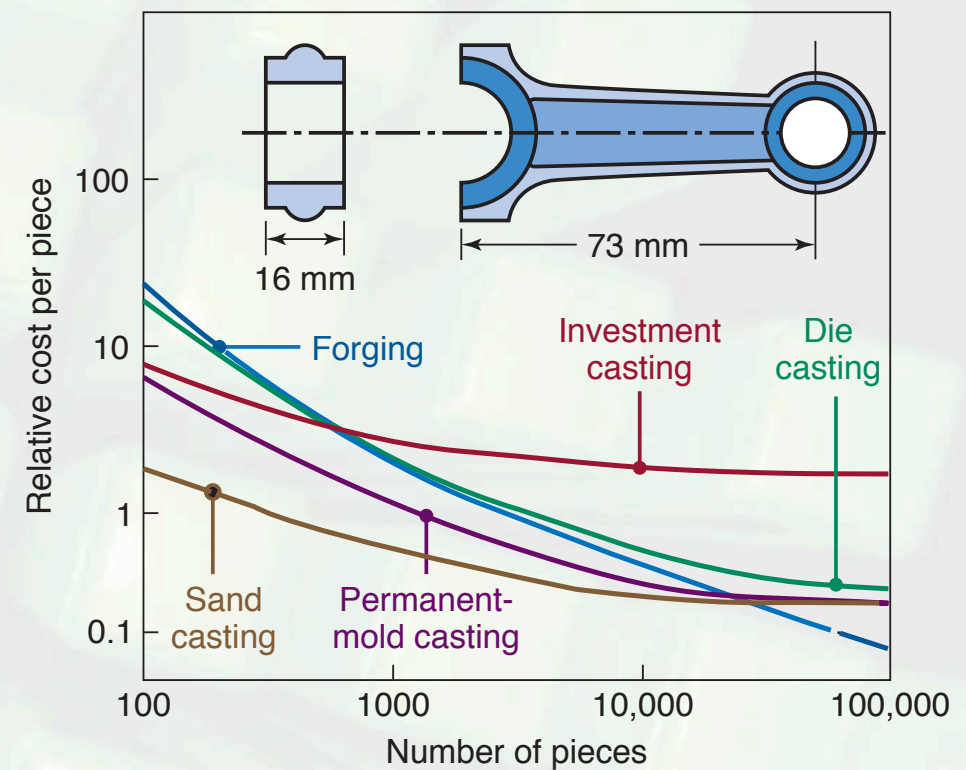
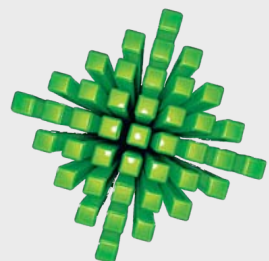


FIGURE 6.72 Relative unit costs of a small connecting rod made by various forging and casting processes. Note that, for large quantities, forging is more economical. Sand casting is the more economical process for fewer than about 20,000 pieces.

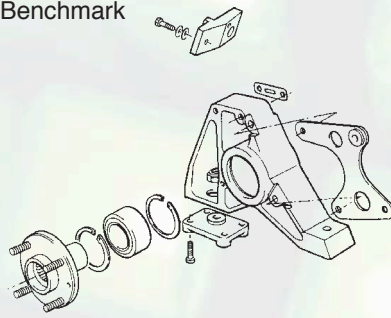
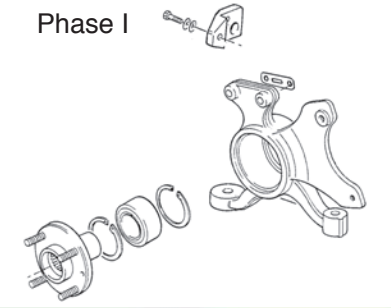
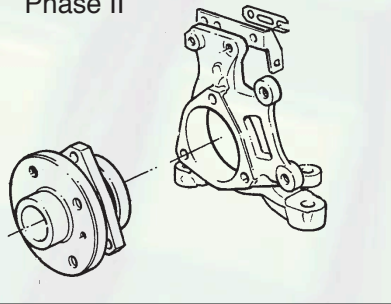


Case Study:Automobile Suspension Uprights



FIGURE 6.73 The Lotus Elise Series 2 Sportscar.
Source: Courtesy of Fox Valley Motorcars.

TABLE 6.4 Vertical suspension uprights in the Lotus Elise Series 2 automobile.

Identification	Description	Mass (kg)	Cost (\$)
	Aluminum extrusion, steel bracket, bushing and housing	2.105	85
	Forged steel	2.685 (+28%)	27.7 (-67%)
	Forged steel	2.493 (+18%)	30.8 (-64%)

